https://doi.org/10.3799/dqkx.2018.148

新疆东天山玉海西岩体地球化学特征及其地质意义

黄宝强[1],陈寿波[1],李 琛[1],田庆磊[1],王 超[1],吴见新[1],陈明霞[1],韩金生[2],王云峰[2,3*]

1.新疆维吾尔自治区有色地质勘查局七〇四队,新疆哈密 839000
2.中国科学院广州地球化学研究所矿物学与成矿学重点实验室,广东广州 510640
3.中国科学院大学,北京 100049

摘要:玉海西Mo矿位于东天山大南湖—头苏泉岛弧带东段,为新疆有色地勘局704队在2015年新发现的钼矿床.矿区出露的岩石主要为石炭系盐池组、新近系葡萄沟组砂砾岩及一套片麻状花岗岩—闪长岩—辉长岩脉复式岩体.LA-ICP-MS锆石U-Pb定年结果显示,玉海西片麻状花岗岩、闪长岩分别侵位于364 Ma和306 Ma.玉海西岩体均具有正的$\varepsilon_{Hf}(t)$(10.5～14.2)和$\varepsilon_{Nd}(t)$(0.9～4.0)值,较低的I_{Sr}(0.703 282～0.704 111)含量,显示新生地壳或亏损地幔来源特征.其中,片麻状花岗岩具有较小的$Mg^{\#}$值(22～27)、Zr/Hf(28～33)、Ti/Zr(10～29)和Ti/Y(94～149)比值,表明其来源于新生下地壳.闪长岩和辉长岩具有较低的SiO_2(47.55%～57.54%)含量,较高的$Mg^{\#}$值(51～59)及Ti/Zr(20～380)、Ti/Zr(246～269)比值,表明其来源于亏损地幔;此外,样品富集LREEs和LILEs(Rb、Sr等),Ce/Pb(6.5～12.0)比值较低,表明有壳源物质的加入.结合区域地质研究成果,表明玉海西片麻状花岗岩来源于新生下地壳的部分熔融,由古亚洲洋向北俯冲引起;闪长岩同样形成于古亚洲洋俯冲阶段,由亏损地幔并混染地壳形成;辉长岩脉来源于亏损地幔的部分熔融并混染地壳成分,形成于碰撞后伸展阶段,晚于闪长岩(306 Ma)侵位.

关键词:玉海西钼矿;东天山;LA-ICP-MS锆石U-Pb定年;地球化学;Sr-Nd-Hf同位素.
中图分类号:P581 **文章编号**:1000－2383(2018)09－2943－23 **收稿日期**:2018－03－03

Geochemical Features and Geological Significance of Yuhaixi Plutons in Eastern Tianshan, Xinjiang

Huang Baoqiang[1], Chen Shoubo[1], Li Chen[1], Tian Qinglei[1], Wang Chao[1], Wu Jianxin[1], Chen Mingxia[1], Han Jinsheng[2], Wang Yunfeng[2,3*]

1.*No.704 Geological Party, Xinjiang Geological Exploration Bureau for Nonferrous Metals, Hami* 839000, *China*
2.*Key Laboratory of Mineralogy and Metallogeny, Guangzhou Institute of Geochemistry, Chinese Academy of Sciences, Guangzhou* 510640, *China*
3.*University of Chinese Academy of Sciences, Beijing* 100049, *China*

Abstract: The Yuhaixi Mo deposit, located in the eastern part of the Dananhu-Tousuquan island arc belt, was discovered by the No.704 Geological Party of Xinjiang Geological Exploration Bureau for Nonferrous Metals in 2015. Rocks occurring at Yuhaixi contain the Carboniferous Yanchi Formation, Neogene Putaogou Formation and felsic-mafic plutons (gneissic granite, granite, diorite and gabbro dike). LA-ICP-MS zircon U-Pb dating reveals that gneissic granite and diorite replaced at ca. 364 Ma and 306 Ma, respectively. Yuhaixi intrusions are characterized by high $\varepsilon_{Hf}(t)$ (10.5－14.2) and $\varepsilon_{Nd}(t)$ (0.9－4.0) values, and low I_{Sr}(0.703 282－0.704 111) values, indicating depleted-mantle or juvenile-crust sources. The gneissic granite is characterized by low $Mg^{\#}$ value (22－27), and Zr/Hf (28－33), Ti/Zr (10－29) and Ti/Y (94－149) ratios, implying a juvenile-crust source. The diorite and the gabbro dike are marked by low Si_2O content (47.55%－57.54%), high $Mg^{\#}$ values (51－59), and Ti/Zr

基金项目:新疆维吾尔自治区地质勘查基金项目(No.T15-3-XJ03).
作者简介:黄宝强(1988－),男,本科,资源勘查工程专业.ORCID: 0000-0002-7503-4315. E-mail: xjyshbq@163.com
*通讯作者:王云峰,ORCID: 0000-0001-6394-0882. E-mail: wangyunnfeng@163.com

引用格式:黄宝强,陈寿波,李琛,等,2018.新疆东天山玉海西岩体地球化学特征及其地质意义.地球科学,43(9):2943－2965.

(20－380) and Ti/Zr (246－269) ratios, which indicate that these rocks were likely formed by the part melting of the depleted mantle. However, diorite and the gabbro dike samples are rich in LREEs and LILEs (e.g., Rb, Sr), with low Ce/Pb ratios (6.5－12.0), suggesting the mixing of crustal component. Combining with the regional geological studies, the Yuhaixi gneissic granite was likely derived from the juvenile low crust, related with the north subduction of the Kangguer ocean plate; the diorite was also formed under a subducion setting by the partial melting of depleted mantle, and mixed with crustal component when it traversed the crust; the gabbro dike was probably derived from the depleted mantle, mixing with crustal component as well, in a post-collisional extension setting, the age of which was latter than 306 Ma.

Key words: Yuhaixi Mo deposit; eastern Tianshan; zircon U-Pb dating; geochemistry; Sr-Nd-Hf isotope.

0 引言

东天山位于中国新疆北部,其包含3个构造带,从北往南依次为:博格达－哈尔里克岛弧带、觉罗塔格带及中天山地块;其中,觉罗塔格带又可划分为大南湖－头苏泉岛弧带、康古尔韧性剪切带、阿齐山－雅满苏带这 3 个构造带(图 1;王京彬等,2006;王京彬和徐新 2006; Qin *et al.*, 2011; Chen *et al.*,

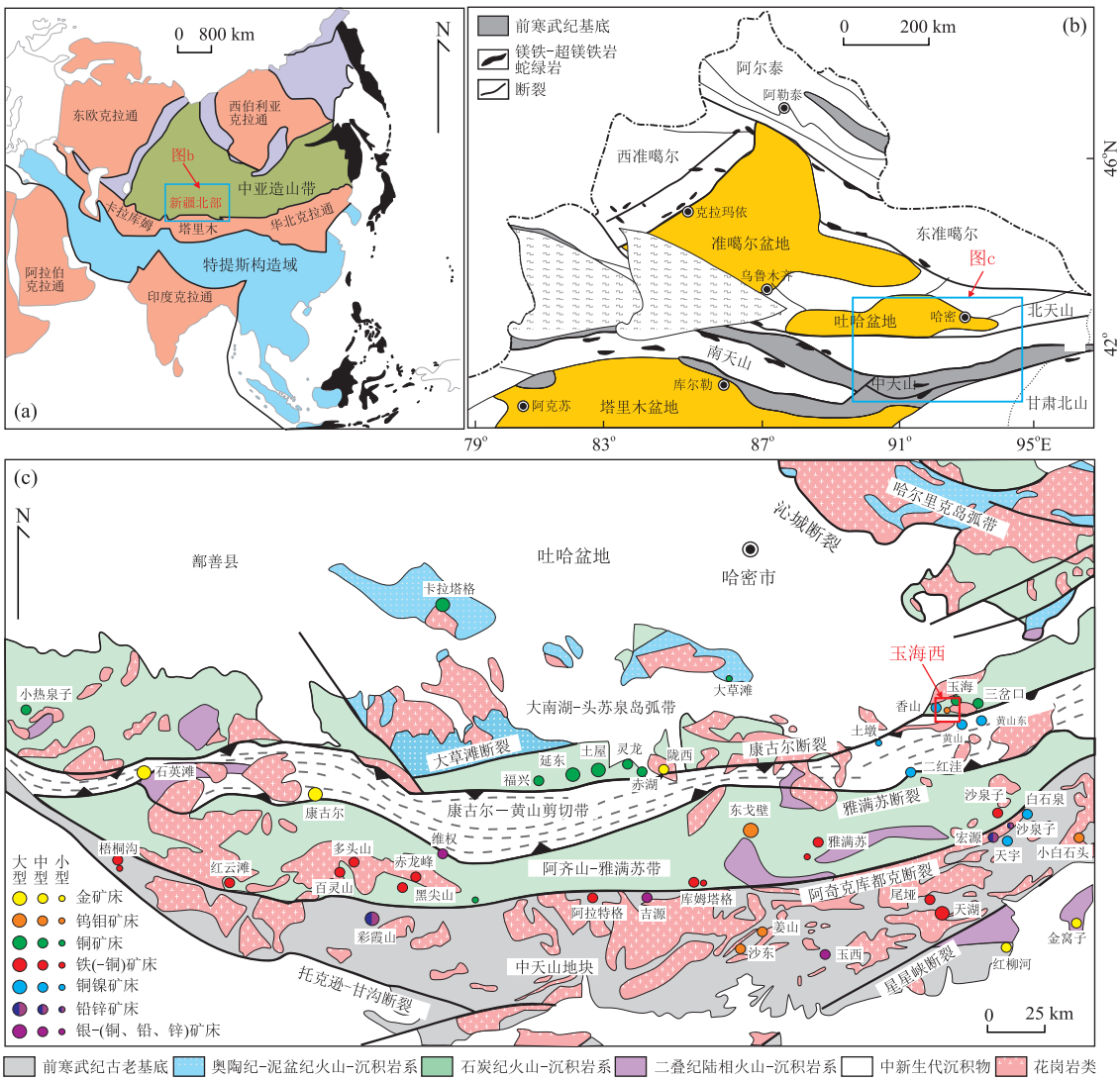

图 1 中亚造山带构造简图(a);新疆北部构造简图(b);东天山地质特征及重要矿床分布(c)

Fig.1 Tectonic sketch of the Central Asian orogenic Belt (a) and northern Xinjiang (b); geological characteristics of the eastern Tianshan belt and major mineral deposit distribution (c)

图 a 据 Wang *et al.*(2018);图 b 据 Chen *et al.*(2012)修改;图 c 据王京彬等(2006)、王京彬和徐新(2006)、Deng *et al.*(2017)修改

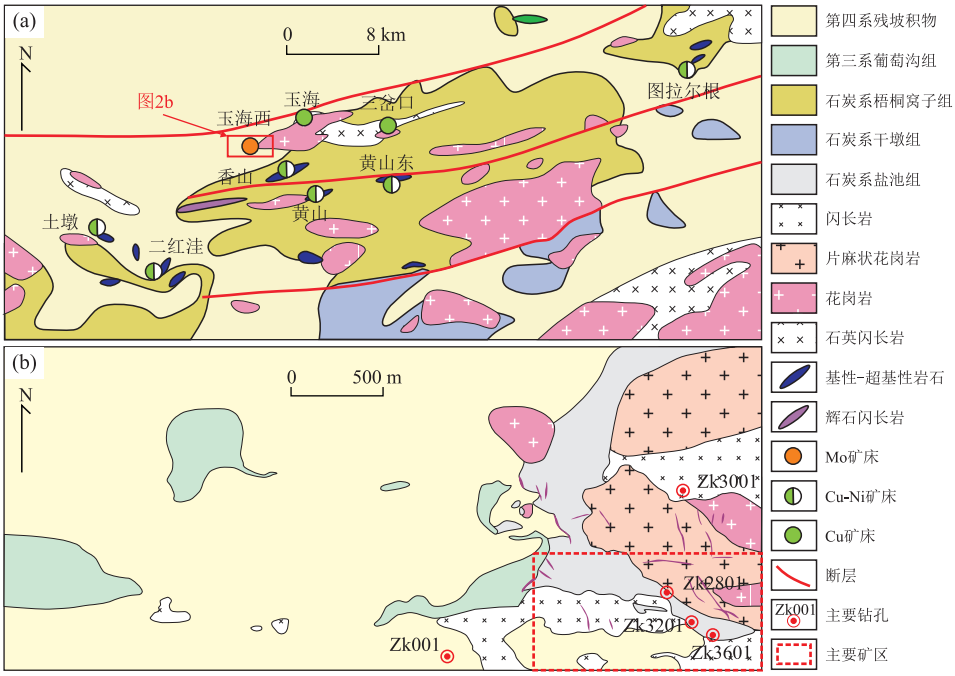

图 2　玉海西矿集区(a)和斑岩 Cu-Mo 矿区(b)地质简图

Fig.2　Geological sketch of the Yuhaixi mineral camp (a) and porphyry Cu-Mo deposit (b)

图 a 据 Wang *et al*.(2016b)修改;图 b 据新疆有色地勘局 704 队,2015,新疆哈密市玉海西铜(钼)矿预查,哈密

2012; Xiao *et al*., 2013).作为中亚造山带的重要组成部分,东天山地区在奥陶纪到三叠纪经历了复杂的构造－岩浆事件及陆壳增生过程(Chen *et al*., 2007, 2012; Pirajno, 2009, 2013; 翟裕生等, 2011),为成矿提供了良好的条件,并使其成为中国重要的 Cu-Fe-Ni-Co-Mo-Au-Ag-W 多金属成矿省(Zhang *et al*., 2004; Chen *et al*., 2012;吴艳爽等, 2013).其中,大南湖－头苏泉岛弧带是该区重要的斑岩 Cu-Mo 成矿带,已发现有土屋－延东、福兴、赤湖、灵龙等多个斑岩 Cu-Mo 矿床(Shen *et al*., 2014a, 2014b; 王云峰等, 2016; Zhang *et al*., 2015; Wang *et al*., 2016c).前人已对该带西部做了大量的研究,主要集中在地质学(芮宗瑶等,2002; Shen *et al*., 2014a, 2014b;王云峰等,2016)、年代学(Xiao *et al*., 2015;肖兵等,2015, 2017; Wang *et al*., 2017)、构造演化及成矿作用(Shen *et al*., 2014a, 2014b; Xiao *et al*., 2015)等方面.然而,该带东部构造－岩浆－成矿作用的相关研究依然薄弱.

近年来,对大南湖－头苏泉岛弧带东段的三岔口 Cu-Mo 矿床及新发现的玉海 Cu-Mo 矿床的研究表明,该区构造－岩浆活动复杂,出露有晚奥陶纪到三叠纪的侵入体,这些岩体与该区成矿有着密切的关系(张照伟等,2016; Wang *et al*., 2016a, 2016b, 2018).然而,在玉海 Cu-Mo 矿床,成矿期辉钼矿的形成年龄约为 350～360 Ma(Wang *et al*., 2016b),与矿区已发现的石英闪长岩(ca. 443 Ma; Wang *et al*., 2018)、花岗岩(ca. 325 Ma; Wang *et al*., 2018)及辉长岩脉(ca. 291 Ma; Wang *et al*., 2018)的结晶年龄均相差甚远;三岔口矿区同样发现有该现象(待发表).这些现象表明,在该区存在一期重要的 Mo 成矿事件,然而相关致矿岩体依然未被发现.因此,有必要对该区岩浆作用及 Mo 成矿作用加大研究,确定 Mo 矿化的致矿岩体及矿化中心,为该区的找矿勘查指明方向.

玉海西钼矿是新疆有色地质勘查局 704 队于 2015 新发现的一处钼矿床.其位于玉海 Cu-Mo 矿床西南侧,距离玉海铜矿约 7 km,距离三岔口 Cu-Mo 矿床约 15 km(图 2a).该区出露的片麻状花岗岩中含有浸染状、细脉浸染状的辉钼矿化,这些特征表明玉海西片麻状花岗岩很可能是该区 Mo 矿化的致矿岩体.本文首次报道了玉海西钼矿矿区岩体的锆石 U-Pb 年龄、全岩元素地球化学特征、Sr-Nd-Hf 同位素特征及辉钼矿 Re-Os 年龄,并结合野外地质调查及室内岩相学测试,详细研究了玉海西钼矿成岩成矿年龄、岩石成因、地球动力学背景及矿床成因,期望能有助于加深对玉海西－玉海－三岔口成矿带矿床成因的理解,为下一步找矿勘查指明方向.

1 区域地质

东天山为乌鲁木齐—库尔勒公路以东,吐哈盆地以南,塔里木盆地以北的天山地区(Zhu *et al*., 2016).构造上,该区在古生代到中生代受古亚洲洋活动的影响(图1;Allen *et al*., 1993; Meng, 2003; Wu *et al*., 2011; Xu *et al*., 2013),经历过多次的俯冲、碰撞造山事件(Xiao *et al*., 2003, 2013; Zhang *et al*., 2008).东天山主要由3部分组成:北部的博格达—哈尔里克岛弧带、中部的觉罗塔格构造带及南部的中天山地块(图1c;Chen *et al*., 2012; Xiao *et al*., 2013; Shen *et al*., 2014a;马星华等,2015).其中,博格达—哈尔里克岛弧带主要由古生代火山沉积岩组成,并有少量的中生代到新生代的沉积岩、火山岩及火山碎屑岩夹层(曹福根等,2006;马星华等,2015).该区分布有古生代的花岗质及镁铁—超镁铁质岩石,并有少量的Cu-Au矿分布(Gao *et al*., 2015; Deng *et al*., 2017).中天山地块主要是由前寒武基底构成,前人在该区已发现了大量的Pb-Zn-(Ag)、Fe、Cu-Ni及Fe-(Ti-V)矿床(王京彬等,2006;李玮等,2016).

觉罗塔格带主要由古生代海相沉积岩、酸—基性火山岩及酸—超基性侵入岩组成(Zhang *et al*., 2003, 2004),可进一步分为3个构造带,从北往南依次为:大南湖—头苏泉岛弧带、康古尔韧性剪切带及阿齐山—雅满苏带(图1c;秦克章等,2002).大南湖—头苏泉岛弧带主要由泥盆纪—石炭纪的火山沉积岩组成,出露地层主要有:泥盆系大南湖组玄武质、安山质火山岩,石炭系干墩组火山沉积岩,石炭系企鹅山群中—基性火山岩、火山碎屑岩及沉积岩,侏罗系沉积岩(刘敏等,2009;郭谦谦等,2010;张达玉等,2010).东天山地区主要的斑岩Cu-Mo矿床均分布在该带之中,如土屋—延东、福兴、赤湖及灵龙.康古尔韧性剪切带出露的地层主要为石炭系干墩组和梧桐窝子组火山沉积岩、石炭系雅满苏组火山岩及火山碎屑岩(Zhang *et al*., 2008;王银宏等,2014),该带中的岩石大部分发生了绿片岩相变质及塑性变形(Shen *et al*., 2014a, 2014b).该带中分布有大量的Au矿(如石英滩等)、Cu-Ni矿(如黄山、黄山东等).阿齐山—雅满苏带出露的地层主要为石炭系雅满苏组双峰式火山岩,石炭系沙泉子组复理岩,石炭系土古土布拉克组碎屑岩、安山质火山灰及碳酸盐岩夹层,二叠系库莱组海相及陆相碎屑沉积岩(花林宝,2001; Hou *et al*., 2014).

东天山地区出露有大量的石炭纪到二叠纪酸性到超基性侵入岩,这些岩体与该区的Cu、Ni、Mo、Fe、Au矿化有着密切的时空关系(Mao *et al*., 2005, 2008;周涛发等,2010; Chen *et al*., 2012).此外,东天山地区分布有大量的近东西向断裂,如大草滩断裂、康古尔断裂、雅满苏及阿奇克库都克—沙泉子断裂(Zhang *et al*., 2008).

2 矿区地质

矿区地层主要为下石炭统盐池组及新近世葡萄沟组(图2b).盐池组主要分布在矿区的东部,出露岩层厚度达300 m,岩性主要为变粒岩、浅粒岩及角闪片岩,岩石多呈灰黑、灰色,具有片状构造.葡萄沟组主要分布于矿区的中部及西部,分布面积较广.主要为钙质、粘土质砂砾岩,产状近于水平,其厚度随地形的增高而增大.矿区内构造单一,以断裂为主,断裂沿北东向分布,其控制着该区岩浆岩分布.

区内中—酸性岩浆岩较为发育,已发现岩体有片麻状花岗岩(图3a,3b)、闪长岩(图3c,3d)、辉长岩脉(图3e,3f)及花岗岩(图3g,3h).片麻状花岗岩分布在矿区的东部(图2b),岩石呈片麻状,矿物均呈定向排列.岩石中黑云母含量在2%～3%,石英含量约为25%,钾长石含量约为45%,斜长石含量约为25%,并有少量的锆石、白云母.花岗岩广泛分布于玉海西、玉海等矿区,玉海西地区的花岗岩侵入早期片麻状花岗岩中(图2b).花岗岩中主要矿物有斜长石(～25%)、石英(～20%)、钾长石(～45%)和黑云母(～8%),并有少量的磷灰石、榍石及锆石等矿物.Wang *et al*.(2018)已得到花岗岩锆石U-Pb年龄为325.4±2.5 Ma.闪长岩主要分布在片麻状花岗岩的东侧及南侧(图2b),岩石中暗色矿物含量约40%,以角闪石和黑云母为主(角闪石∶黑云母≈2∶1);长石含量约为60%,主要为斜长石;石英含量小于3%.此外,磁铁矿的含量在2%～3%.辉长岩脉在矿区呈NW和EW向展布(图2b),宽1～10 m,切穿前期片麻状花岗岩、花岗岩及闪长岩,表明其形成晚于其他岩体.岩脉中角闪石含量约为50%,斜长石含量约为40%,辉石含量约为10%,并有少量的磁铁矿(<3%).辉长岩脉普遍发生不同程度的角闪石化,辉石被角闪石交代,主要呈交代残余结构(图3f).

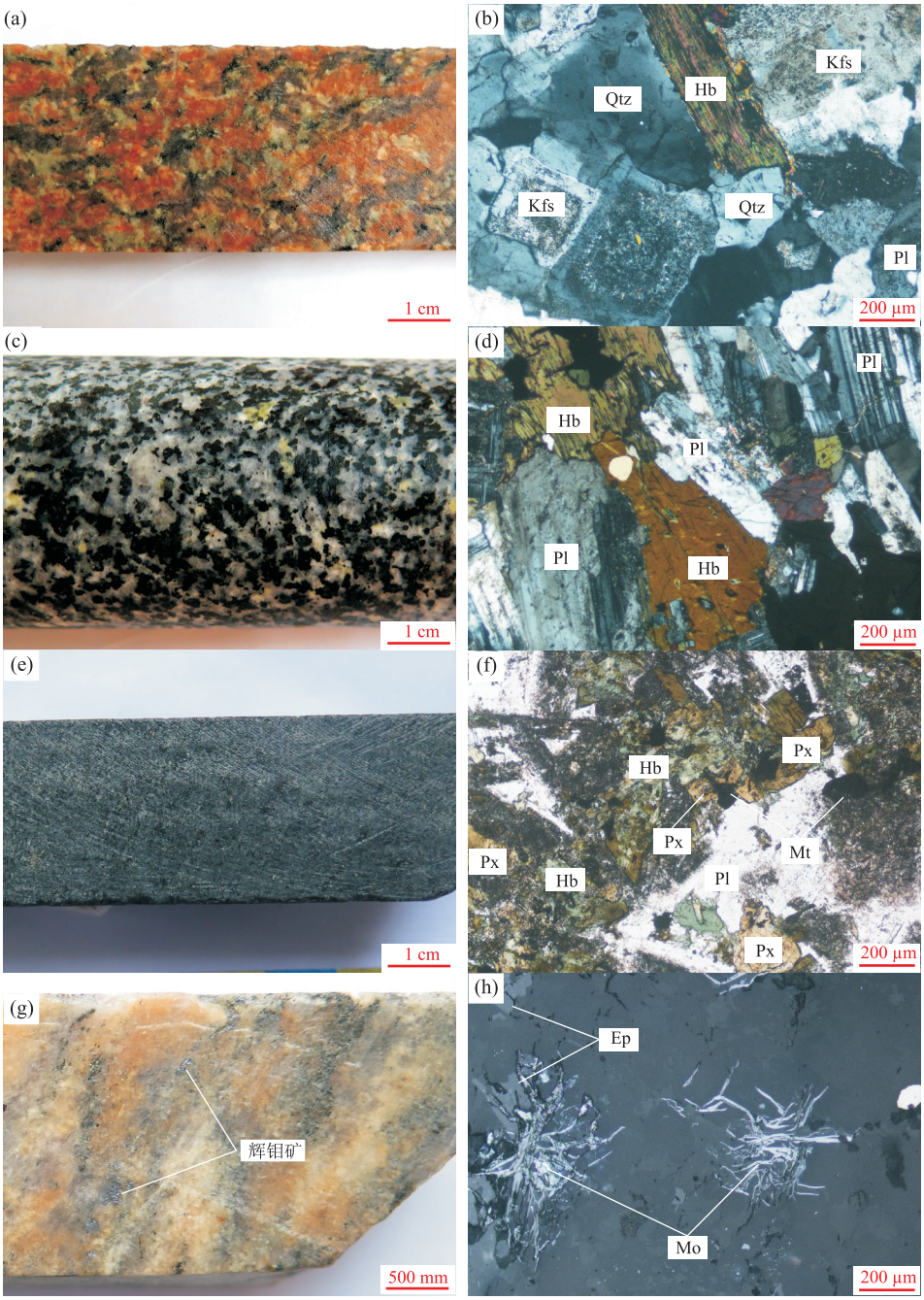

图 3　玉海西矿区主要岩体手标本及镜下照片

Fig.3　Photographs and photomicrographs showing the major rock types of the Yuhaixi deposit

a.片麻状花岗岩手标本;b.片麻状花岗岩正交镜下照片;c.闪长岩手标本;d.闪长岩镜下照片;e.辉长岩脉手标本;f.辉长岩脉镜下照片;g.片麻状花岗岩中辉钼矿化;h.在镜下,辉钼矿与绿帘石化密切相关.Qtz.石英;Hb.角闪石;Pl.斜长石;Kfs.钾长石;Px.辉石;Mo.辉钼矿;Mt.磁铁矿;Ep.绿帘石

3　分析方法

锆石等矿物分选是在河北廊坊市诚信地质服务有限公司完成.样品经过破碎、常规浮选和磁选分离后,在双面镜下对锆石进行分选,将晶型好、无明显裂隙和包裹体的锆石挑出,用环氧树脂制靶.锆石经打磨抛光后,进行反射光、透射光显微镜照相和阴极发光(CL)分析.锆石 U-Pb 同位素年龄及锆石微量元素分析是在中山大学广东省海洋资源与近岸工程重点实验室完成.测试仪器为电感耦合等离子体质谱仪(Agilent 7700X)和准分子激光剥蚀系统(GeoLasPro)联机,激光器为 ArF 准分子激光器.激光剥蚀束斑直径为 32 μm,激光能量密度为 5 J/cm^2,剥蚀频率为 5 Hz.实验中采用 He 作为剥蚀物质的载

气,Ar 为辅助气.锆石年龄计算采用标准锆石 91500(1 062 Ma)为外标,标准锆石 Plesovice(337 Ma)为监控盲样.元素含量采用国际标样 NIST 610 作为外标,Si 为内标元素进行校正.每 5 个样品测试之间分析两次年龄标样 91500,每 10 个样品之间分析 2 次微量标样 NIST 610.锆石元素含量及 U-Th-Pb 同位素比值及年龄计算采用软件 ICPMSDataCal 完成,样品的 U-Pb 年龄谐和图绘制及加权平均年龄计算由 ISOPLOT 完成.

锆石 Lu-Hf 同位素测试是在中科院广州地球化学研究所同位素地球化学国家重点实验室进行,所用仪器为 RESOlution M-50 激光剥蚀系统(Thermo Scientific,德国)及 Neptune Plus(Resonetics,德国)多接收器电感耦合等离子质谱仪(MC-ICP-MS).分析中所用的激光束斑为 44 μm,频率为 8 Hz,能量为 15 J/cm^2.该试验以 Penglai 锆石为标样,其$^{176}Hf/^{177}Hf=0.282\ 888\pm0.000\ 024$(2SD).$\varepsilon_{Hf}(t)$根据每个测试点的锆石 U-Pb 年龄计算而来,计算方法见 Bouvier *et al.*(2008),该过程中采用的^{176}Lu 衰变常数为 1.867×10^{-11} a^{-1}(Söderlund *et al.*, 2004).锆石 Hf 单阶段模式年龄(T_{DM})及两阶段模式年龄(T_{DM2})分别根据 Griffin *et al.*(2002, 2004)的方法计算而来.

岩石主量元素分析是在广州澳实分析检测有限公司完成;微量及稀土元素地球化学分析在贵州星月测试科技有限公司完成.主量元素分析使用 Rikagu RIX 2100 型 X 荧光光谱仪(XRF)完成,分析精度优于 1%,具体过程见 Zhou *et al.*(2014);微量元素分析使用 Cetac ASX-510 型电感耦合等离子质谱仪(ICP-MS)完成,分析精度优于 5%,详细步骤见 Li *et al.*(2005).

全岩 Sr-Nd 同位素比值分析在贵州星月测试科技有限公司完成,Nd 同位素测试是用 Nu Plasma HR 型多接受电感耦合等离子质谱仪(MC-ICP-MS)完成;Sr 同位素测试是用 VG Sector 54 热电离质谱仪(TIMS)上完成.Sr 和 Nd 同位素比值分别用$^{86}Sr/^{88}Sr=0.119\ 4$ 和$^{146}Nd/^{144}Nd=0.721\ 9$ 来校正.在分析过程中,分别以 NBS-987 和 JNdi-1 为 Sr 和 Nd 的标样来对样品进行标定.具体分析过程见 Collerson *et al.*(2002).

4 分析结果

4.1 锆石 U-Pb 年龄

玉海西片麻状花岗岩中,锆石多为无色透明晶体,粒径多为200～400μm,长宽比在1∶1～1∶5;

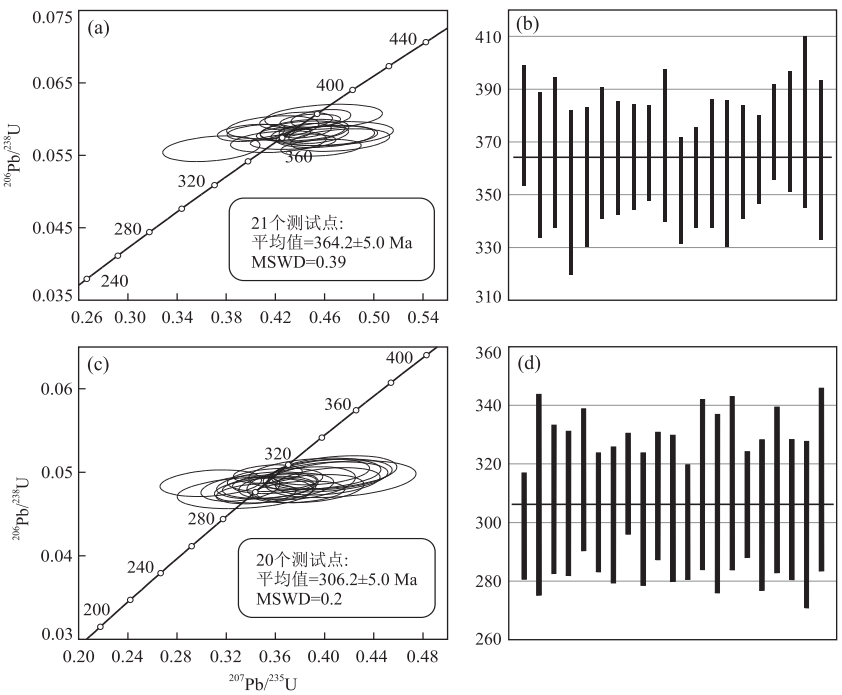

图 4 玉海西岩体锆石 U-Pb 年龄谐和图

Fig.4 U-Pb concordia and weighted average diagrams of the zircons of the Yuhaixi intrusions

a,b.片麻状花岗岩;c,d.闪长岩

表 1　玉海西岩体 LA-ICP-MS 锆石 U-Pb 定年结果

Table 1　Results of LA-ICP-MS U-Pb dating for Yuhaixi intrusions

分析号	元素含量(10^{-6})		Th/U	同位素比值				年龄(Ma)			
	Th	U		$^{207}Pb/^{235}U$	1σ	$^{206}Pb/^{238}U$	1σ	$^{207}Pb/^{235}U$	1σ	$^{206}Pb/^{238}U$	1σ
样品 S001-2,片麻状花岗岩,21 个点											
S001-2-2	132	228	0.58	0.344 2	0.026 5	0.047 4	0.001 0	300.4	20.0	298.8	6.1
S001-2-4	42	83	0.51	0.413 1	0.050 1	0.049 2	0.001 8	351.1	36.0	309.5	11.1
S001-2-5	53	102	0.52	0.402 6	0.034 8	0.048 9	0.001 3	343.5	25.2	307.9	8.2
S001-2-6	47	91	0.51	0.307 5	0.033 8	0.048 7	0.001 3	272.2	26.2	306.5	8.0
S001-2-7	61	103	0.60	0.397 2	0.032 3	0.050 0	0.001 3	339.6	23.4	314.6	7.7
S001-2-8	81	146	0.55	0.354 3	0.030 5	0.048 2	0.001 1	307.9	22.8	303.5	6.7
S001-2-9	49	119	0.41	0.331 6	0.026 4	0.048 1	0.001 2	290.8	20.1	302.6	7.7
S001-2-11	151	260	0.58	0.353 8	0.022 9	0.049 8	0.000 9	307.6	17.2	313.3	5.5
S001-2-12	39	109	0.35	0.351 7	0.033 7	0.047 8	0.001 2	306.0	25.3	301.2	7.5
S001-2-13	58	137	0.42	0.359 8	0.031 7	0.049 1	0.001 1	312.1	23.7	309.0	7.0
S001-2-14	20	86	0.24	0.353 6	0.033 8	0.048 4	0.001 3	307.5	25.4	304.9	8.2
S001-2-15	102	162	0.63	0.378 9	0.030 9	0.047 7	0.001 1	326.2	22.7	300.1	6.5
S001-2-16	94	156	0.60	0.404 6	0.041 1	0.049 7	0.001 5	345.0	29.7	312.9	9.3
S001-2-17	35	72	0.48	0.381 0	0.036 1	0.048 7	0.001 6	327.8	26.6	306.4	9.9
S001-2-19	22	72	0.31	0.392 0	0.044 0	0.049 8	0.001 5	335.9	32.1	313.4	9.4
S001-2-20	107	174	0.62	0.359 4	0.028 1	0.048 6	0.001 0	311.8	21.0	306.1	5.9
S001-2-21	69	111	0.63	0.388 2	0.035 8	0.048 0	0.001 4	333.1	26.2	302.5	8.5
S001-2-24	40	107	0.37	0.400 9	0.041 4	0.049 4	0.001 5	342.3	30.0	311.1	9.1
S001-2-25	77	115	0.67	0.368 8	0.031 5	0.048 4	0.001 3	318.8	23.4	304.4	7.9
S001-2-28	25	63	0.40	0.335 3	0.045 0	0.047 5	0.001 5	293.6	34.3	299.3	9.5
S001-2-30	15	88	0.17	0.407 7	0.041 8	0.050 0	0.001 6	347.2	30.1	314.6	9.9
样品 S3601-16,闪长岩,20 个点											
S3601-16-1	404	1 064	0.38	0.457 0	0.019 9	0.060 1	0.001 0	382.2	13.9	376.3	6.1
S3601-16-2	63	148	0.42	0.460 6	0.032 8	0.057 6	0.001 3	384.7	22.8	361.1	7.6
S3601-16-3	113	247	0.46	0.443 8	0.029 5	0.058 4	0.001 3	372.9	20.7	365.9	7.8
S3601-16-4	42	133	0.32	0.367 9	0.032 3	0.055 9	0.001 4	318.1	24.0	350.7	8.8
S3601-16-5	96	255	0.38	0.422 6	0.031 9	0.056 9	0.001 2	357.9	22.8	356.6	7.4
S3601-16-6	126	342	0.37	0.442 3	0.028 2	0.058 4	0.001 1	371.9	19.9	365.7	6.8
S3601-16-9	154	372	0.42	0.400 0	0.022 2	0.058 1	0.001 0	341.7	16.1	364.0	5.9
S3601-16-10	151	435	0.35	0.408 3	0.022 6	0.058 2	0.000 9	347.6	16.3	364.4	5.5
S3601-16-12	347	981	0.35	0.444 3	0.017 4	0.058 4	0.000 8	373.3	12.2	365.9	5.0
S3601-16-15	110	249	0.44	0.417 9	0.030 7	0.058 9	0.001 3	354.6	22.0	368.8	7.9
S3601-16-17	153	335	0.46	0.457 2	0.026 7	0.056 0	0.000 9	382.3	18.6	351.5	5.8
S3601-16-18	160	341	0.47	0.434 5	0.028 4	0.056 9	0.000 9	366.4	20.1	356.7	5.3
S3601-16-20	73	174	0.42	0.463 2	0.032 7	0.057 7	0.001 1	386.5	22.7	361.6	6.8
S3601-16-22	160	272	0.59	0.472 7	0.032 9	0.057 1	0.001 3	393.1	22.7	358.0	7.7
S3601-16-23	471	1 139	0.41	0.455 1	0.019 9	0.057 8	0.001 0	380.9	13.9	362.5	5.9
S3601-16-24	500	1 140	0.44	0.426 5	0.018 0	0.058 0	0.000 8	360.7	12.8	363.2	4.6
S3601-16-25	280	932	0.30	0.448 3	0.020 1	0.059 7	0.000 8	376.1	14.1	373.9	4.8
S3601-16-26	146	436	0.33	0.436 8	0.024 3	0.059 7	0.001 0	368.0	17.2	374.1	6.1
S3601-16-29	97	165	0.59	0.459 3	0.039 1	0.060 3	0.001 4	383.8	27.2	377.5	8.6
S3601-16-30	45	118	0.38	0.466 2	0.040 7	0.058 0	0.001 4	388.6	28.2	363.3	8.3

阴极发光(CL)图像显示,玉海西片麻状花岗岩样品中(S3601-16)锆石均呈现清晰的振荡环带;Th/U 比值分别为 0.30～0.59,表明其为岩浆锆石.LA-ICP-MS 定年显示,玉海西花岗岩的锆石$^{206}Pb/^{238}U$年龄为 350.7～377.5 Ma,加权平均年龄为 364.2±5.0 Ma(MSWD=0.39)(图 4a,4b).玉海西闪长岩中,锆石为透明晶体,粒径为 100～200 μm,长宽比为 1∶1～1∶2;在 CL 图像中,玉海西闪长岩样品(S001-2)中锆石均呈现清晰的振荡环带;Th/U 比值为 0.17～0.67(主要为 0.4～0.6),显示其岩浆成因.LA-ICP-MS 定年显示,玉海西闪长岩的锆石$^{206}Pb/^{238}U$年龄为 298.8～314.6 Ma,加权平均年龄为 306.2±5.0 Ma(MSWD=0.2)(图 4c,4d).锆石 U-Pb 同位素测试结果及相应的锆石微量元素结果分别见表 1 和表 2.

4.2　全岩地球化学

选取无明显蚀变或蚀变较轻的玉海西片麻状花岗岩、闪长岩和辉长岩脉样品进行全岩主、微量元素

表 2 玉海西岩体锆石微量元量含量(10^{-6})

Table 2 Zircon trace elements (10^{-6}) results of the Yuhaixi intrusions

点号	La	Ce	Pr	Nd	Sm	Eu	Gd	Tb	Dy	Ho	Er	Tm	Yb	Lu
S001-2,片麻状花岗岩,21 个点														
S001-2-2		12.08	0.066	1.98	4.84	0.97	29.02	8.18	102.81	36.35	172.75	35.33	400.93	69.81
S001-2-4	0.009	7.37	0.013	0.54	1.32	0.60	8.78	3.62	45.35	17.23	83.63	17.48	203.93	36.89
S001-2-5		7.78	0.033	1.09	2.71	0.59	14.27	4.25	52.99	20.57	97.21	21.16	235.78	40.93
S001-2-6	0.018	8.41	0.055	1.07	3.25	0.56	15.76	5.06	60.34	21.36	107.12	22.60	255.80	43.76
S001-2-7	0.051	10.01	0.129	4.17	5.94	1.11	24.28	7.33	80.34	29.25	137.36	28.02	311.93	52.15
S001-2-8		9.99	0.059	1.85	3.87	0.92	22.44	6.82	83.29	29.47	141.65	29.09	333.38	58.14
S001-2-9	0.019	8.22	0.025	0.21	0.96	0.25	10.19	3.47	47.11	19.31	97.62	21.29	257.90	43.00
S001-2-11		11.10	0.048	1.47	3.66	0.92	24.82	7.43	94.17	34.26	170.36	36.83	453.46	77.49
S001-2-12		8.22	0.006	0.10	1.40	0.22	8.64	3.60	47.10	18.26	95.61	20.74	254.85	46.85
S001-2-13	0.019	9.19	0.033	0.00	1.93	0.21	8.17	3.06	41.51	16.46	86.22	17.81	211.63	38.84
S001-2-14		2.85	0.006	0.49	0.19	0.18	2.46	0.89	11.21	4.91	28.26	7.13	100.85	21.15
S001-2-15		11.20	0.032	0.86	5.19	1.10	28.32	7.85	99.20	36.14	171.54	34.94	381.33	64.19
S001-2-16		10.62	0.067	0.61	3.83	0.74	19.78	6.39	78.68	28.17	136.00	29.15	328.37	57.43
S001-2-17		7.07	0.061	0.15	1.39	0.46	9.81	3.26	41.99	14.54	73.65	15.48	180.40	33.78
S001-2-19		3.67	0.000	0.59	0.96	0.30	4.23	1.77	22.22	8.65	44.78	10.39	124.04	25.26
S001-2-20	0.242	11.45	0.170	3.64	6.46	1.11	29.86	8.41	106.36	37.74	180.53	35.77	400.74	70.21
S001-2-21		10.73	0.000	0.95	2.45	0.47	20.10	5.70	79.70	29.58	138.73	28.93	320.87	54.35
S001-2-24		7.01	0.000	0.37	1.74	0.34	6.49	2.56	33.87	14.48	75.44	17.04	202.95	38.44
S001-2-25		11.08	0.101	2.95	5.01	1.24	27.81	7.84	96.61	33.29	156.76	30.01	332.07	56.55
S001-2-28		5.95	0.014	0.17	1.60	0.31	6.53	2.22	28.51	10.75	58.65	12.18	146.03	26.76
S001-2-30		2.93	0.000	0.00	0.29	0.13	2.38	0.62	9.39	4.19	25.54	6.41	97.87	22.34
S3601-16,闪长岩,20 个点														
S3601-16-1	0.459	68.19	0.440	4.94	8.15	1.90	40.52	16.10	235.26	98.90	504.12	109.12	1 262.05	214.87
S3601-16-2	0.021	20.63	0.021	0.93	2.80	0.83	14.49	5.61	75.00	31.30	156.24	35.48	421.35	78.49
S3601-16-3		34.07	0.099	0.77	2.38	1.18	18.00	6.49	90.86	36.96	192.91	42.13	497.53	88.47
S3601-16-4		13.63	0.034	0.40	0.83	0.31	7.89	3.47	49.84	21.10	113.92	25.99	317.82	58.98
S3601-16-5		20.45	0.036	0.48	2.23	0.85	15.58	6.53	86.93	36.35	189.95	41.49	505.07	91.27
S3601-16-6	0.066	22.98	0.015	0.74	2.81	1.05	14.98	7.37	101.57	41.81	213.76	45.39	556.74	98.54
S3601-16-9		46.50	0.046	0.60	3.56	1.03	22.70	9.99	137.30	58.65	300.74	65.75	789.20	139.06
S3601-16-10	0.304	32.46	0.488	2.95	3.79	0.75	15.84	6.94	95.45	39.41	201.16	44.66	520.03	89.80
S3601-16-12		44.87	0.058	1.02	4.30	1.11	31.23	13.39	185.48	78.62	391.59	84.73	999.13	170.49
S3601-16-15	0.010	21.66	0.046	1.21	4.72	1.61	24.64	8.96	117.23	44.43	223.51	48.25	548.08	96.51
S3601-16-17		26.63	0.019	0.42	1.55	0.76	14.39	5.50	79.89	32.29	156.44	34.78	404.52	69.65
S3601-16-18	0.092	34.24	0.225	3.10	5.56	1.51	33.17	11.70	161.42	64.13	326.89	70.59	808.03	137.57
S3601-16-20	1.022	20.54	0.511	2.53	3.58	1.14	18.59	6.74	100.55	38.49	191.19	40.92	470.30	85.06
S3601-16-22	1.774	38.80	2.793	25.33	16.58	3.45	51.49	11.18	131.84	46.89	226.94	49.63	571.07	100.80
S3601-16-23	6.820	113.82	11.976	70.30	50.55	4.06	111.35	32.53	341.60	114.31	534.26	112.91	1237.84	208.19
S3601-16-24		69.67	0.035	0.88	3.79	1.20	50.27	21.35	320.04	131.44	681.02	143.76	1639.95	276.30
S3601-16-25	0.397	30.59	0.220	2.88	5.29	0.66	30.42	12.63	190.47	79.74	419.40	91.23	1042.88	181.10
S3601-16-26		23.22	0.048	0.58	1.94	0.50	15.64	6.41	92.63	38.12	195.72	42.64	502.04	91.03
S3601-16-29	0.119	28.15	0.272	4.64	6.26	1.31	29.04	9.89	114.38	41.67	205.64	43.01	488.72	86.46
S3601-16-30		15.21	0.026	0.67	1.26	0.38	10.54	3.92	59.27	22.79	124.85	27.87	329.85	60.84

分析,分析结果见表 3.玉海西片麻状花岗岩有较高的 SiO_2(72.93%～75.65%)、Na_2O(2.91%～4.19%)和 K_2O(3.90%～5.32%)含量,较低的 Al_2O_3(12.48%～14.27%)、$Fe_2O_3^T$(1.54%～1.89%)、MgO(0.24%～0.35%)和 CaO(1.26%～1.40%)含量.闪长岩具有较低的 SiO_2(53.79%～57.54%)和 K_2O(1.12%～1.53%)含量,较高的 Al_2O_3(16.77%～17.86%)、Na_2O(3.84%～4.26%)、$Fe_2O_3^T$(7.41%～8.49%)、MgO(4.14%～4.52%)和 CaO(6.97%～7.78%)含量.辉长岩脉中,

表 3　玉海西岩体主(%)、微量元素(10^{-6})含量

Table 3　Whole rock major (%) and trace (10^{-6}) elements of Yuhaixi intrusions

样号	片麻状花岗岩			闪长岩			辉长岩脉		
	S3601-16	S3201-26	S3201-20	S001-1	S001-2	S001-3	S3201-11	S3201-11-1	S3201-12
SiO_2	75.65	72.93	75.04	57.54	54.64	53.79	48.22	47.55	48.96
Al_2O_3	12.48	14.27	13.70	16.77	17.42	17.86	16.36	16.38	16.06
K_2O	4.86	5.32	3.90	1.23	1.53	1.12	0.93	1.11	1.02
Na_2O	2.91	3.45	4.19	3.84	4.01	4.26	2.88	2.58	2.92
CaO	1.28	1.40	1.26	6.97	7.18	7.78	9.51	8.84	9.22
$Fe_2O_3^T$	1.67	1.89	1.54	7.41	8.13	8.49	10.73	11.00	10.62
MgO	0.24	0.35	0.28	4.14	4.32	4.52	7.71	8.03	7.84
MnO	0.08	0.09	0.10	0.14	0.18	0.17	0.23	0.24	0.24
P_2O_5	0.04	0.06	0.04	0.20	0.26	0.28	0.41	0.41	0.38
TiO_2	0.16	0.19	0.11	0.86	1.00	1.02	1.10	1.10	1.02
LOI	0.48	0.67	0.41	0.68	1.20	0.63	2.16	2.47	2.20
Total	99.85	100.62	100.57	99.78	99.87	99.92	100.24	99.71	100.48
Na_2O+K_2O	7.77	8.77	8.09	5.07	5.54	5.38	3.81	3.69	3.94
K_2O/Na_2O	1.67	1.54	0.93	0.32	0.38	0.26	0.32	0.43	0.35
$Mg^{\#}$	22	27	26	53	51	51	59	59	59
A/CNK	1.01	1.02	1.02	0.83	0.82	0.80	0.71	0.76	0.71
A/NK	1.24	1.25	1.23	2.19	2.11	2.17	2.85	3.01	2.72
Rb	47.5	69.9	58.6	26.1	29.1	21.1	20.4	24.7	22.6
Ba	1 020	786	816	377	558	404	151	185	164
Th	3.970	4.470	6.270	0.575	1.560	1.78	0.284	0.325	0.307
U	1.210	1.020	2.770	0.283	0.803	0.715	0.155	0.155	0.160
Nb	4.77	7.04	5.30	4.67	5.31	5.29	2.76	2.78	2.64
Ta	0.26	0.42	0.64	0.28	0.31	0.30	0.13	0.14	0.13
K	40 328	44 145	32 362	10 206	12 696	9 294	7 717	9 211	8 464
La	17.40	19.90	16.90	12.70	14.40	16.50	8.92	9.05	8.85
Ce	33.40	38.90	30.80	31.20	37.20	42.40	24.60	25.00	24.20
Pb	11.90	15.40	13.10	4.82	4.69	4.23	2.30	2.08	2.35
Pr	3.70	4.32	3.22	4.38	5.32	6.01	3.81	3.88	3.72
Sr	191	203	289	671	694	746	522	466	479
Nd	12.80	14.90	10.40	18.90	22.80	25.70	18.10	18.30	17.50
P	175	262	175	873	1 135	1 223	1 790	1 790	1 659
Sm	2.10	2.56	1.64	4.35	4.92	5.48	4.48	4.57	4.34
Zr	42.2	36.0	63.0	13.5	15.5	15.4	30.5	25.7	25.2
Hf	1.29	1.23	2.11	0.78	0.88	0.90	1.01	0.91	0.92
Eu	0.72	0.73	0.38	0.99	1.26	1.37	1.49	1.48	1.43
Ti	842	1 050	619	5 060	5 730	5 850	6 380	6 400	5 900
Gd	1.55	1.88	1.20	3.97	4.31	4.77	4.48	4.56	4.32
Tb	0.20	0.25	0.17	0.60	0.63	0.70	0.68	0.69	0.66
Dy	1.05	1.31	0.951	3.48	3.63	4.00	4.03	4.10	3.90
Y	5.80	7.06	6.60	20.40	21.50	23.80	23.70	23.90	22.80
Ho	0.21	0.25	0.20	0.71	0.75	0.83	0.86	0.86	0.83
Er	0.56	0.65	0.57	2.00	2.09	2.31	2.39	2.39	2.29
Tm	0.08	0.09	0.09	0.30	0.32	0.36	0.36	0.36	0.35
Yb	0.56	0.61	0.67	1.95	2.10	2.31	2.31	2.31	2.22
Lu	0.088	0.095	0.11	0.28	0.32	0.35	0.34	0.34	0.33
Co	1.33	2.73	1.32	23.00	25.90	25.70	35.20	37.70	34.50
Ni	1.29	1.68	1.40	33.60	36.10	36.30	89.70	95.50	94.40
Cr	12.3	13.3	18.7	59.3	73.8	96.8	504.0	524.0	537.0
ΣREE	51.01	58.80	47.70	43.90	51.60	58.90	37.33	37.93	40.67
$(La/Yb)_N$	22.29	23.48	18.15	4.67	4.92	5.12	2.77	2.81	2.86
$(Tb/Yb)_N$	1.64	1.90	1.18	1.41	1.37	1.38	1.34	1.37	1.35
$(La/Sm)_N$	5.35	5.02	6.65	1.88	1.89	1.94	1.29	1.28	1.32
Eu^*	1.22	1.02	0.82	0.73	0.84	0.82	1.02	0.99	1.01

SiO_2、Al_2O_3、Na_2O、K_2O、$Fe_2O_3^T$、CaO 和 MgO 的含量分别是 47.55%～48.96%、16.06%～16.38%、2.58%～2.92%、0.93%～1.11%、10.73%～11.00%、8.84%～9.22%和 7.71%～8.03%.玉海西岩石样品全碱(Na_2O+K_2O)含量为 3.69%～8.77%,在图 5a 中,片麻状花岗岩落入花岗岩区域,闪长岩落入闪长岩和辉长闪长岩区域,辉长岩脉落入辉长岩区域.在图 5b 中,花岗岩落入高钾钙碱性系列到钾玄岩系列区域,而闪长岩及辉长岩脉落入中钾钙碱型系列.此外,玉海西岩体的铝饱和指数(A/CNK)为 0.71～1.02,显示偏铝质特征(图 5c).

玉海西岩体稀土含量均较低,为 37.33×10^{-6}～58.80×10^{-6}.在稀土元素球粒陨石标准化配分图中,片麻状花岗岩轻重稀土分异明显,$(La/Yb)_N$ 为 18.15～23.48,δEu 的值为 0.82～1.22(图 6a);闪长岩配分曲线右倾,较为富集重稀土,$(La/Yb)_N$ 为 4.67～5.12,有弱的 Eu 负异常($\delta Eu=0.73$～0.84)(图 6c);辉长岩脉具有弱的轻稀土富集、重稀土亏损,$(La/Yb)_N$ 为 2.77～2.86,无明显 Eu 亏损($\delta Eu=0.99$～1.02)(图 6e).在微量元素原始地幔标准化图解中,片麻状花岗岩明显富集 Rb、Ba、U、K 和 Pb 等大离子亲石元素,亏损 Nb、Ta、Nd 和 Ti 等高场强元素,但无明显的 Zr、Hf 亏损(图 6b).闪长岩及辉长岩脉样品相对富集 Rb、Ba、U、La、Pb 等大离子亲石元素,亏损 Nb、Ta、Zr、Hf 及 Ti 等高场强元素(图 6d,6f).

4.3 锆石 Hf 同位素

玉海西岩体锆石 Hf 同位素测试是在 U-Pb 定年的基础上进行的,笔者分别选取 10 颗片麻状花岗岩锆石和 10 颗闪长岩锆石进行锆石 Hf 同位素测试(图 7a).片麻状花岗岩锆石测试点 $^{176}Hf/^{177}Hf$ 变化范围为 0.282 865～0.282 955 之间,对应的 $\varepsilon_{Hf}(t)$ 值为 10.8～14.2,其锆石 Hf 单阶段模式年龄(T_{DM})为 424～549 Ma,两阶段模式年龄(T_{DM_2})为 458～667 Ma.闪长岩锆石中 $^{176}Hf/^{177}Hf$ 值为 0.282 884～0.282 947,$\varepsilon_{Hf}(t)$ 值为 10.9～12.6,对应的 Hf 单阶段模式年龄(T_{DM})为 430～517 Ma,两阶段模式年龄(T_{DM_2})为 509～647 Ma.玉海西片麻状花岗岩、闪长岩锆石 Hf 同位素分析结果见表 4.

4.4 全岩 Sr-Nd 同位素

玉海西岩体全岩 Rb-Sr、Sm-Nd 同位素数据见表 5.片麻状花岗岩、闪长岩及辉长岩脉的 I_{Sr} 值分别为 0.703 282～0.703 776、0.703 668～0.704 111 及 0.703 610～0.703 644(图 7b).片麻状花岗岩的 $\varepsilon_{Nd}(t)$ 值为 3.56～4.03,单阶段模式年龄为 705～765 Ma,两阶段模式年龄为 786～824 Ma;闪长岩的 $\varepsilon_{Nd}(t)$ 值为 1.47～1.95,单阶段模式年龄为 985～1 128 Ma,两阶段模式年龄为 908～947 Ma;辉长岩脉的 $\varepsilon_{Nd}(t)$ 值为 0.90～1.06,单阶段模式年龄为 1 305～1 342 Ma,两

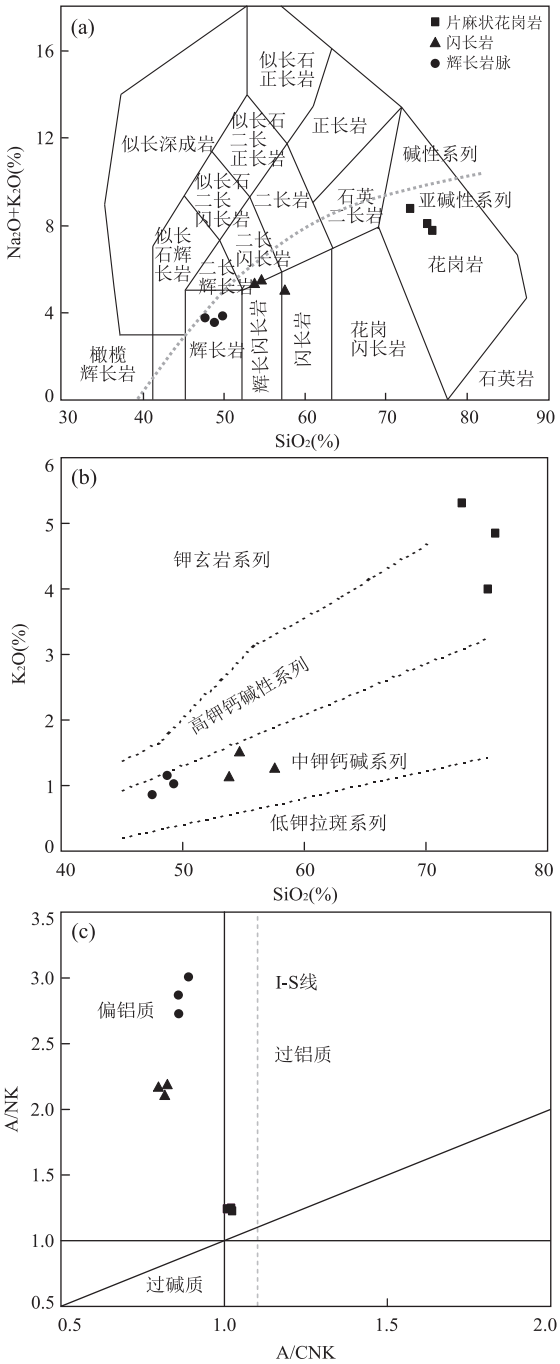

图 5 玉海西岩体 N_2O+K_2O vs. SiO_2 图解(a),K_2O vs. SiO_2 图解(b)以及 A/NK vs. A/CNK 图解(c)

Fig.5 N_2O+K_2O vs. SiO_2 diagram (a), K_2O vs. SiO_2 diagram (b) and A/NK vs. A/CNK diagram (c) for the Yuhaixi intrusions

图 a 据 Peccerillo and Taylor(1976);图 b 据 Maniar and Piccoli(1989)

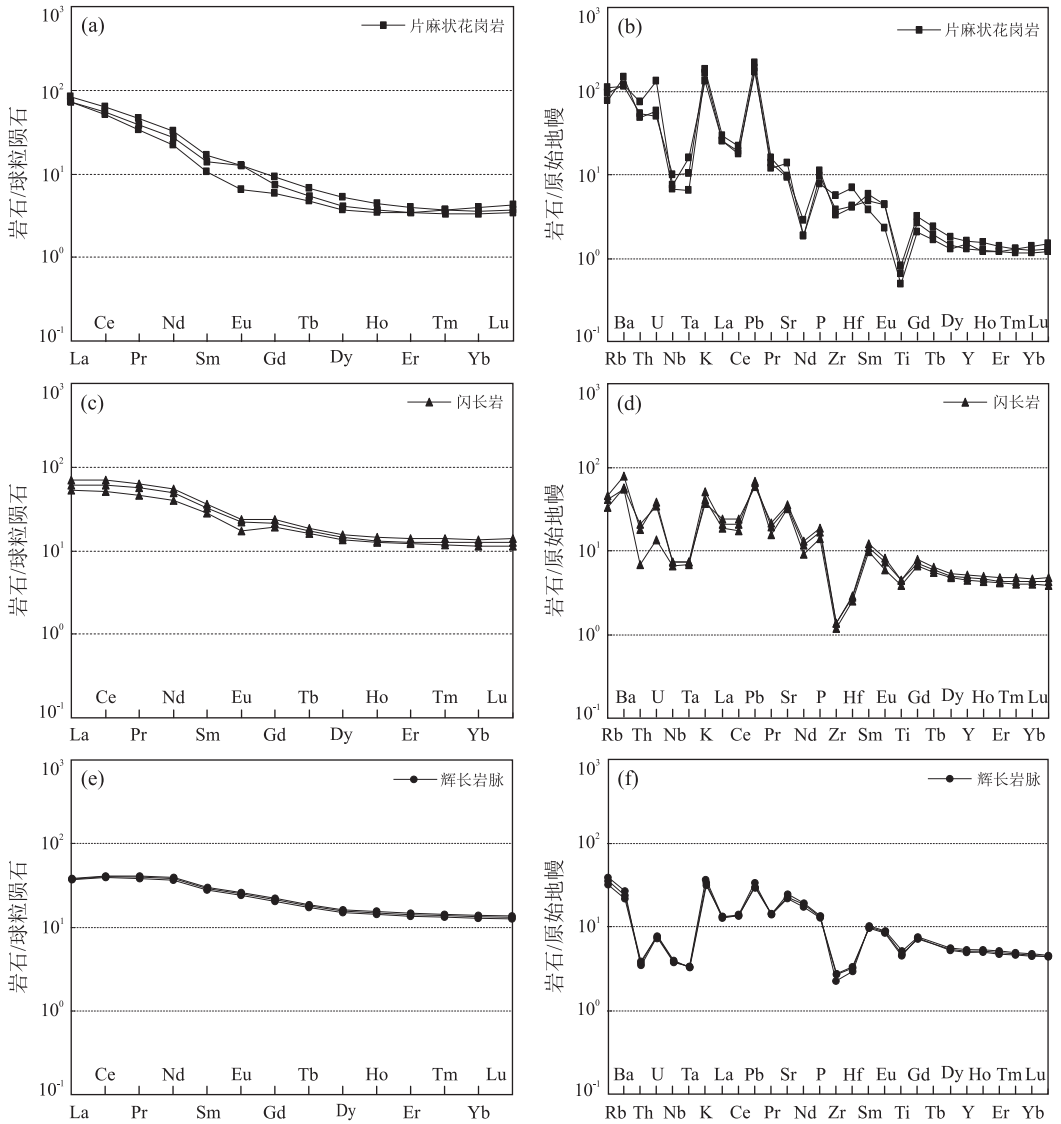

图 6　玉海西岩体球粒陨石标准化 REE 模式(a、c、e)和原始地幔标准化微量元素蛛网图(b、d、f)

Fig.6　Chondrite-normalized REE (a, c, e) and primitive-mantle-normalized trace elements diagrams for Yuhaixi intrusions (b, d, f)

据 Sun and McDonough(1989)

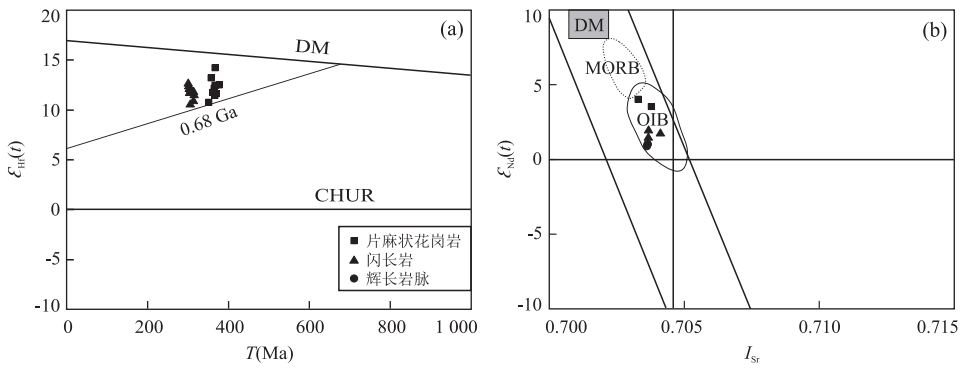

图 7　玉海西岩体 I_{Sr}-$\varepsilon_{Nd}(t)$图解(a)及锆石 $\varepsilon_{Hf}(t)$ vs. U-Pb 年龄(b)图解

Fig.7　I_{Sr}-$\varepsilon_{Nd}(t)$ (a) and zircon $\varepsilon_{Hf}(t)$ vs. U-Pb ages (b) diagrams for the Yuhaixi intrusions

图 a 据 Morris and Hart(1983);图 b 据 Arculus and Powell(1986)

表4 玉海西岩体锆石Hf同位素值

Table 4 Zircon Hf isotopes of Yuhaixi intrusions

样品号	年龄(Ma)	$^{176}Yb/^{177}Hf$	1σ	$^{176}Lu/^{177}Hf$	1σ	$^{176}Hf/^{177}Hf$	1σ	$\varepsilon_{Hf}(0)$	$\varepsilon_{Hf}(t)$	T_{DM}(Ma)	T_{DM2}(Ma)	$f_{Lu/Hf}$
样品S001-2,片麻状花岗岩,10个点												
S001-2-2	376.3	0.074 947	0.000 445	0.002 975	0.000 016	0.282 912	—	5.0	12.5	508	576	−0.91
S001-2-5	361.1	0.029 499	0.000 233	0.001 205	0.000 006	0.282 888	—	4.1	11.8	519	612	−0.96
S001-2-6	365.9	0.029 753	0.000 465	0.001 240	0.000 018	0.282 955	—	6.5	14.2	424	458	−0.96
S001-2-11	350.7	0.022 884	0.000 076	0.000 957	0.000 002	0.282 865	—	3.3	10.8	549	667	−0.97
S001-2-17	356.6	0.047 433	0.000 272	0.001 901	0.000 012	0.282 936	—	5.8	13.2	458	515	−0.94
S001-2-19	365.7	0.044 243	0.000 628	0.001 784	0.000 021	0.282 881	—	3.8	11.5	537	634	−0.95
S001-2-21	364.0	0.035 883	0.000 053	0.001 486	0.000 002	0.282 900	—	4.5	12.2	505	587	−0.96
S001-2-24	364.4	0.045 994	0.000 236	0.001 829	0.000 011	0.282 895	—	4.4	11.9	517	603	−0.94
S001-2-25	365.9	0.070 392	0.000 333	0.002 785	0.000 010	0.282 916	—	5.1	12.5	500	570	−0.92
S001-2-28	368.8	0.050 052	0.000 619	0.001 980	0.000 020	0.282 885	—	4.0	11.6	534	626	−0.94
样品S3601-16,闪长岩,10个点												
S3601-16-4	314.6	0.022 314	0.000 107	0.000 868	0.000 005	0.282 905	—	4.7	11.5	489	595	−0.97
S3601-16-5	303.5	0.019 014	0.000 060	0.000 750	0.000 001	0.282 917	—	5.1	11.7	471	573	−0.98
S3601-16-6	302.6	0.014 597	0.000 056	0.000 599	0.000 001	0.282 929	—	5.5	12.1	453	546	−0.98
S3601-16-9	313.3	0.023 379	0.000 093	0.000 913	0.000 002	0.282 915	—	5.1	11.8	476	574	−0.97
S3601-16-10	301.2	0.013 627	0.000 087	0.000 556	0.000 003	0.282 937	—	5.8	12.4	441	527	−0.98
S3601-16-15	309.0	0.013 162	0.000 077	0.000 526	0.000 002	0.282 917	—	5.1	11.8	469	568	−0.98
S3601-16-17	304.9	0.015 455	0.000 519	0.000 629	0.000 019	0.282 884	—	4.0	10.5	517	647	−0.98
S3601-16-26	300.1	0.021 888	0.000 104	0.000 824	0.000 001	0.282 947	—	6.2	12.6	430	509	−0.98
S3601-16-29	312.9	0.011 583	0.000 047	0.000 472	0.000 001	0.282 887	—	4.1	10.9	510	632	−0.99
S3601-16-30	306.4	0.019 577	0.000 062	0.000 748	0.000 004	0.282 922	—	5.3	11.9	464	560	−0.98

表5 玉海西岩体全岩Sr-Nd同位素

Table 5 Whole rock Sr-Nd isotopes of Yuhaixi intrusions

样号	岩性	年龄(Ma)	Rb (10^{-6})	Sr (10^{-6})	$^{87}Rb/^{86}Sr$	$^{87}Sr/^{86}Sr$	I_{Sr}	Sm (10^{-6})	Nd (10^{-6})	$^{147}Sm/^{144}Nd$	$^{143}Nd/^{144}Nd$	$\varepsilon_{Nd}(0)$	$\varepsilon_{Nd}(t)$	T_{DM}(Ma)	T_{DM2}(Ma)
S3201-20	片麻状花岗岩	364	58.6	289	0.586 601	0.70 632 220	0.703 282	1.64	10.4	0.095 334	0.512 603	−0.68	4.03	705	786
S3201-26		364	69.9	203	0.996 404	0.70 893 905	0.703 776	2.56	14.9	0.103 870	0.512 599	−0.76	3.56	765	824
S001-1	闪长岩	306	26.1	671	0.112 504	0.70 415 823	0.703 668	4.35	18.9	0.139 143	0.512 598	−0.78	1.47	1 128	947
S001-2		306	29.1	694	0.121 284	0.70 463 893	0.704 111	4.92	22.8	0.130 456	0.512 595	−0.84	1.75	1 016	924
S001-3		306	21.1	746	0.081 807	0.70 403 246	0.703 676	5.48	25.7	0.128 909	0.512 602	−0.70	1.95	985	908
S3201-11	辉长岩脉	291	20.4	522	0.113 034	0.70 411 156	0.703 644	4.48	18.1	0.149 636	0.512 601	−0.72	1.03	1 305	970
S3201-11-1		291	24.7	466	0.153 308	0.70 424 492	0.703 610	4.57	18.3	0.150 973	0.512 597	−0.80	0.90	1 342	981
S3201-12		291	22.6	479	0.136 466	0.70 419 776	0.703 633	4.34	17.5	0.149 930	0.512 603	−0.68	1.06	1 306	968

阶段模式年龄为 968～981 Ma.

5　讨论

5.1　成岩与成矿年龄

近些年来,大南湖－头苏泉岛弧带东段构造演化及成矿作用已成为东天山地区的研究重点,并已取得了一系列可喜的成果.张照伟等(2016)得到玉海铜矿含矿岩石的年龄为 422.3±4.0 Ma;王超等(2015)得到三岔口岩体年龄为 443 Ma;Wang *et al*.(2016a)在三岔口矿区得到其长英质侵入体的年龄为 440～426 Ma;Wang *et al*.(2016b)得到玉海矿区闪长岩年龄为 441.6±2.5 Ma,石英闪长岩年龄为 430.3±2.6 Ma;Wang *et al*.(2018)得到玉海石英闪长岩年龄为 443.5±4.1 Ma.这些研究表明,大南湖－头苏泉岛弧带形成于早古生代,而非一些学者认为的晚古生代活动大陆边缘弧(李文明等,2002;芮宗瑶等,2002;王京彬和徐新,2006).哈尔里克岛弧带和大南湖－头苏泉岛弧带中已发现的早古生代岩浆岩具有相似的 $\varepsilon_{Hf}(t)$(8.9～19.6;肖兵等,2015;Wang *et al*., 2016a)、$\varepsilon_{Nd}(t)$(4.1～4.9;肖兵等,2015;马星华等,2015)及 $(^{87}Sr/^{86}Sr)_i$ 值(0.703 2～0.704 5;肖兵等,2015;马星华等,2015),且均具有岛弧特征,这表明两个岛弧带在早古生代可能为统一岛弧(曹福根等,2006;郭华春等,2006;马星华等,2015; Wang *et al*., 2018).此外,前人通过对克拉麦里蛇绿岩带之上的沉积序列研究表明,准噶尔东部为主动大陆边缘,而南部的哈尔里克区域却为被动大陆边缘(李华芹,2004;李超等,2009);地震学研究表明,哈尔里克地区莫霍面及以下地幔向北倾斜,表明该区发生了向北俯冲(李华芹等,2006).由此表明,早古生代大南湖－头苏泉岛弧带和哈尔里克岛弧带可能是由古亚洲洋向北俯冲形成的.前人的研究表明,在大南湖－头苏泉岛弧带的西段,有大量的 340～320 Ma 中－酸性岩体出露,并伴随形成了一系列斑岩铜矿(如土屋－延东、赤湖、福兴等),使该带成为了东天山地区重要的斑岩 Cu-Mo 成矿带(Shen *et al*., 2014a, 2014b; Xiao *et al*., 2015; Wang *et al*., 2016c; Zhang *et al*., 2016a).而大南湖－头苏泉岛弧带的东段,在 340～320 Ma 期间只形成了玉海花岗岩(Wang *et al*., 2018)及三岔口东花岗闪长岩(323.2±2.4 Ma;王超等,2015)和花岗岩(321.3±2.5 Ma;王超等,2015),且在这些岩体中未发现 Cu-Mo 矿化.这可能与这些岩体起源于新生下地壳(Wang *et al*., 2018)相关,而西段与斑岩 Cu-Mo 矿化相关的岩体均源自于俯冲板片的部分熔融(Xiao *et al*., 2015; Wang *et al*., 2016c).此外,李华芹等(2004)报道了三岔口铜矿含矿斜长花岗斑岩的年龄为 278±4 Ma; Wang *et al*.(2018)获得玉海辉长岩脉的年龄为 291±3 Ma,并指出其可能形成于碰撞后伸展环境下亏损地幔的部分熔融(Wang *et al*., 2018).这些研究表明,该区经历了古亚洲洋早古生代大洋俯冲到晚古生代碰撞后伸展的完整过程,对于研究东天山地区构造演化过程具有重要意义,同时也是成矿的有利位置.然而,玉海辉钼矿年龄(Wang *et al*., 2016b)及三岔口辉钼矿年龄(待发表)均集中在 360～350 Ma,且在矿区并未发现同期岩浆岩.

笔者所得玉海西片麻状花岗岩年龄(364.2±5.0 Ma)与玉海、三岔口矿区辉钼矿年龄在误差范围内一致,且片麻状花岗岩内有浸染状辉钼矿化(图 3g,3h),这些特征暗示了玉海西片麻状花岗岩可能与区域上 Mo 矿化存在成因联系.前人研究表明,大南湖－头苏泉岛弧带碰撞发生在晚石炭纪到早二叠纪(Xiao *et al*., 2004; Wang *et al*., 2018),而玉海西闪长岩(306.2±5.0 Ma)恰好形成于该时期,这对于碰撞时间的进一步限定有着重要的意义.

5.2　岩石成因

玉海西片麻状花岗岩具有较高的 SiO_2 和 K_2O+Na_2O 含量,较低的 Al_2O_3 含量,在岩体中未见到白云母、电气石及石榴子石等富铝质矿物,同时 I_{Sr}(0.703 282～0.703 776)较低.这些特征表明该岩体可能为 I 或 A 型花岗岩(Chappell *et al*., 1974; Barbarin, 1999).此外,片麻状花岗岩样品含有较低的 Zr 含量及 $10^4\times Ga/Al$ 含量,与 A 型花岗岩特征不符(图 8).因此,玉海西片麻状花岗岩可能为 I 型花岗岩(Whalen *et al*., 1987; Wu *et al*., 2002).此外,玉海西片麻状花岗岩样品具有较高的 LREEs、LILEs 含量,较低的 HREEs、HFSEs 含量.在图 9 中,玉海西片麻状花岗岩具有与火山弧花岗岩相似的特征,表明其可能形成于俯冲环境.

玉海西片麻状花岗岩样品具有较高的 $\varepsilon_{Hf}(t)$(10.8～14.2)和 $\varepsilon_{Nd}(t)$(3.6～4.0),较低的 I_{Sr}(0.703 282～0.703 776),表明其可能形成于新生地壳或者亏损地幔(Shen *et al*., 2017; Wang *et al*., 2018).但实验岩石学已经证明,无论熔融程度多低,地幔橄榄岩都不可能直接形成 SiO_2 含量大于 66%的酸性岩(Jahn and Zhang, 1984),因此片麻状

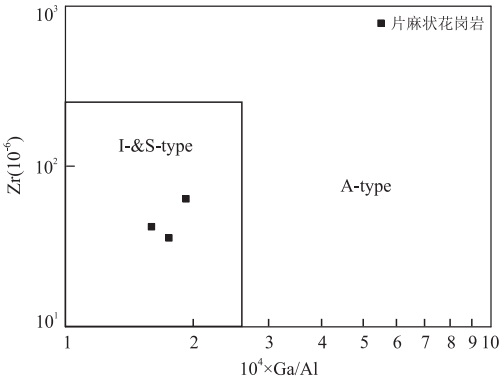

图 8 玉海西片麻状花岗岩 Zr vs. $10^4\times Ga/Al$ 相关图解

Fig.8 Zr vs. $10^4\times Ga/Al$ diagram for Yuhaixi gneissic granite

据 Whalen *et al*.(1987)

花岗岩(SiO_2:72.93%～75.65%)必然形成于新生地壳.俯冲环境下,新生玄武质下地壳(McKenzie, 1989; Vervoort and Blichert-Toft, 1999; Miškovic and Schaltegger, 2009; Zhang *et al*., 2016b)及俯冲板块部分熔融(Zhang *et al*., 2006; Richards and Kerrich, 2007; Xiao *et al*., 2015)均能形成具有类似同位素特征的酸性岩.$Mg^{\#}$ 可作为判断是否有幔源岩浆混合的重要指标.一般来说,由玄武质下地壳部分熔融形成的岩浆岩,无论其熔融程度如何,其 $Mg^{\#}$ 均小于 40,当有地幔物质加入时,$Mg^{\#}$ 才会大于 40(Rapp and Watson, 1995; Smithies and Champion, 2000);而由于板片部分熔融形成的岩浆通过地幔楔时常有地幔物质的加入,因此 $Mg^{\#}$ 通常大于 40(Xiao *et al*., 2015).玉海西片麻岩中,$Mg^{\#}$ 值为 22～27,明显小于 40,表明其可能形成于新生玄武质下地壳的部分熔融.Zr、Hf 均为高场强元素,不同的岩浆源区有着各自不同的 Zr/Hf 比值,地幔中 Zr/Hf 比值约为 50,而地壳中 Zr/Hf 比值约为 36(Anderson, 1983).样品中 Zr/Hf 比值为 28～33,指示岩浆可能来源于下地壳,没有明显幔源物质的加入.此外,较低的 Ti/Zr(10～29;幔源物质中>30;Wedepohl, 1995)、Ti/Y(94～149;幔源物质中>200;Wedepohl, 1995)比值及 Ni(1.3×10^{-6}～1.7×10^{-6};地壳中<47×10^{-6};Anderson, 1983; Rudnick and Gao, 2003)、Cr(12.3×10^{-6}～18.7×10^{-6};地壳中<92×10^{-6}; Anderson, 1983; Rudnick and Gao, 2003)含量等特征同样表明幔源物质加入不明显.

玉海西闪长岩具有较低的 SiO_2(53.79%～57.54%)含量,较高的 MgO 含量(4.14%～4.52%)、$Mg^{\#}$ 值(51～53)及 Ti/Zr(370～380)、Ti/Zr(246～267)比值.在图 7b 中,玉海西闪长岩样品显示正的 $\varepsilon_{Nd}(t)$ 和较低的 $(^{87}Sr/^{86}Sr)_i$ 值;并具有正的 $\varepsilon_{Hf}(t)$ 值,在图 7a 中,落在地幔演化线附近.这些特征均说明玉海西闪长岩可能源自于亏损地幔的部分熔融.在图 10a 上,玉海西闪长岩显示部分熔融特征.然而,玉海西闪长岩样品中富集 LREEs、LILEs,亏损 HREEs、HFSEs,较高的 $(La/Yb)_N$ 比值(4.7～5.1)、较低的 Ce/Pb 比值(6.5～10.2;地壳值为 4～15,地幔值为 25±5;Hofmann, 1997; Rudnick and Gao, 2003)以及较低的 Ni(33.6×10^{-6}～36.3×10^{-6})、Cr(59.3×10^{-6}～96.8×10^{-6})含量,均显示其具有地壳混染的特征.Plank and Langmuir (1998)指出由板片脱水流体交代过的源区形成的岩浆,通常具有较高的 Ba 含量及 Ba/Th 比值(>170).玉海闪长岩样品具有较高的 Ba 含量(377×10^{-6}～558×10^{-6})、Ba/Th 比值(227～656),表明玉海西闪长岩可能来自于受俯冲板片脱

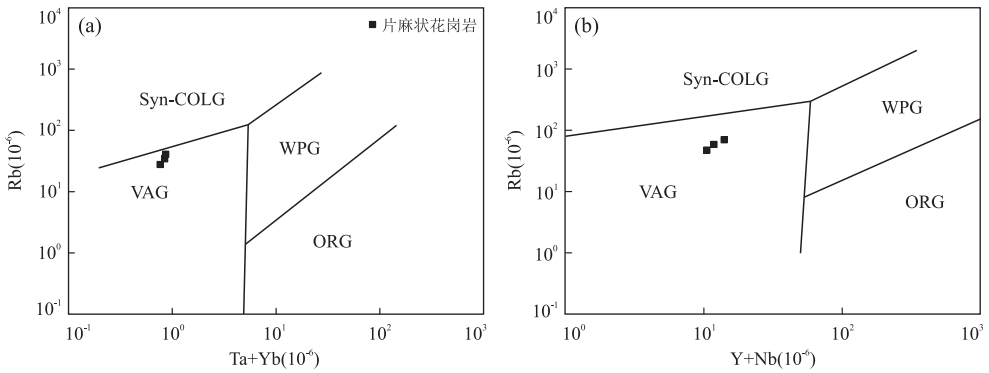

图 9 玉海西片麻状花岗岩构造判别图解

Fig.9 Tectonic discrimination diagrams for the Yuhaixi gnenissic granite

a.Rb vs. Ta+Yb 图解;b.Rb vs. Y+Nb 图解;据 Pearce *et al*.(1984).VAG.火山弧花岗岩类;Syn-COLG.同碰撞花岗岩类;WPG.板内花岗岩类;ORG.洋中脊花岗岩类

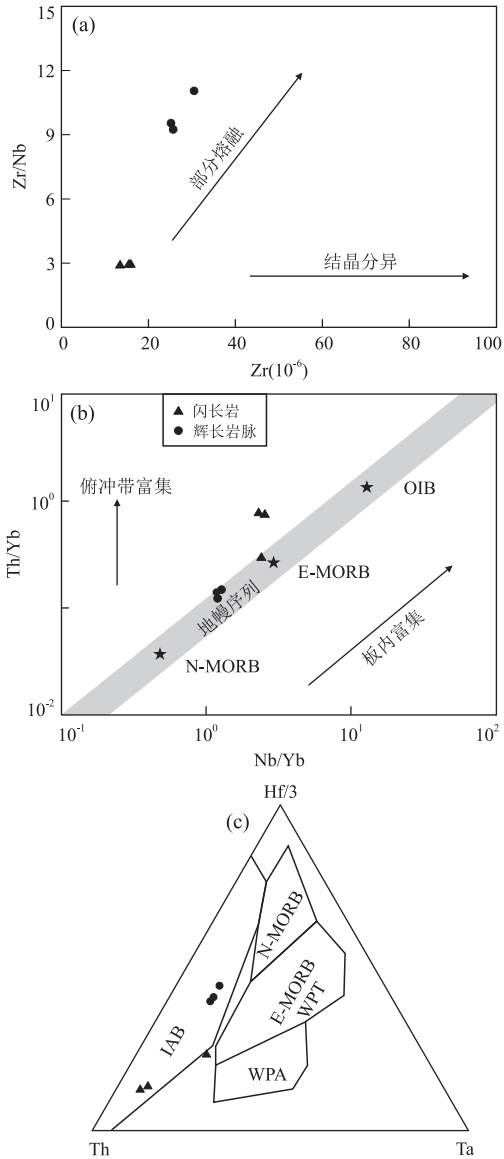

图 10　玉海西岩体 Zr/Nb vs. Zr (a)、Th/Yb vs. Nb/Yb (b)及 Hf/3-Th-Ta(c)相关图解

Fig.10　Zr/Nb vs. Zr (a), Th/Yb vs. Nb/Yb (b) and Hf/3-Th-Ta diagrams for Yuhaixi intrusions

IAB.岛弧玄武岩;WPA.板内拉斑玄武岩;WPT.碱性板内玄武岩;图 a 据 Pearce and Peate(1995);图 b 据 Wang *et al*.(2016b);图 c 据 Harris *et al*.(1986)

水流体交代过的地幔楔的部分熔融(图 11),并在上升过程中有壳源物质的加入.

与闪长岩相似,玉海西辉长岩脉同样具有较低的 SiO_2(47.55%～48.96%)含量,较高的 MgO 含量(7.71%～8.03%)、$Mg^{\#}$ 值(～59)及 Ti/Zr(209～249)、Ti/Zr(259～269)比值,正的 $\varepsilon_{Nd}(t)$(0.90～1.06)和较低的 $(^{87}Sr/^{86}Sr)_i$(0.703 610～0.703 644)值,显示亏损地幔来源.此外,其含有较高的 Ni(89.7×10⁻⁶～95.5×10⁻⁶)、Cr(504×10⁻⁶～537×10⁻⁶)含量,较高的 Nb/Ta 比值(19.7～20.6;地幔约为 17.5,地壳约为 11～12;Green, 1995),同样指示地幔源区.由于辉长岩脉样品相对富集 Rb、U、La、K 和 Pb 等大离子亲石元素,表明岩浆可能混有地壳物质.样品中较低的 Ta/U(0.84～0.87;地壳中约为 0.65,地幔中约为 2.7;Hofmann, 1997; Rudnick and Gao, 2003)和 Ce/Pb(10.3～12.0;地壳中约为 4～15,地幔中约为 25±5;Hofmann, 1997; Rudnick and Gao, 2003)比值说明了地壳成分对辉长岩脉的形成具有重要的作用.此外,样品具有较高的 Ba 含量(151×10⁻⁶～185×10⁻⁶)及 Ba/Th 比值(532～569),表明玉海西辉长岩脉源区可能受到了板片脱水流体的交代(图 11),这也使得岩石的 $\varepsilon_{Nd}(t)$ 值有所降低.研究表明,东天山地区晚古生代镁铁－超镁铁质岩石(约 310～270 Ma)多显示富集 LREEs 和 LILEs(Sr、Ba 等)、亏损 HREEs 和 HFSEs(Nb、Ta 和 Ti 等)、较高的 $\varepsilon_{Nd}(t)$ 值(－1～7.1)和较低的 $(^{87}Sr/^{86}Sr)_i$ 值(0.703 80～0.706 91)的特征,显示亏损地幔源区,并有壳源物质加入(Zhang *et al*., 2003; Wang *et al*., 2018).这些特征与玉海西辉长岩脉相似,表明其可能有相似的源区.综上所述,认为玉海西辉长岩脉源于受俯冲板片脱水流体交代的亏损地幔,并有壳源物质加入.

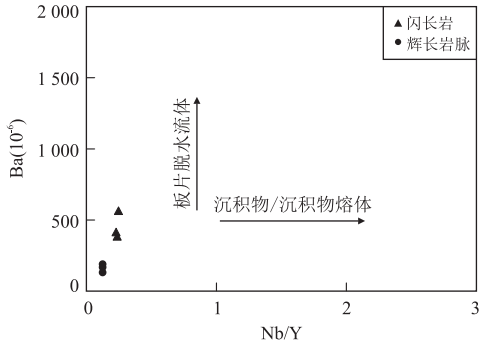

图 11　玉海西岩体 Ba vs. Nb/Y 相关图解

Fig.11　Ba vs. Nb/Y diagram for Yuhaixi intrusions

据 Kepezhinskas *et al*.(1997)

5.3　Nd-Hf 同位素解耦现象

表 1 和表 2 显示,玉海西闪长岩具有较低的 $\varepsilon_{Nd}(t)$ 值(1.47～1.95),相应的 Nd 模式年龄为 985～1 128 Ma;而具有较高的锆石 $\varepsilon_{Hf}(t)$ 值(10.5～12.6),对应的 Hf 模式年龄为 430～517 Ma,明显较 Nd 模式年龄年轻.根据地壳 Nd-Hf 同位素相关性阵列 $\varepsilon_{Hf}(t)=1.34\times\varepsilon_{Nd}(t)+2.82$(Vervoort *et al*., 1999)计算,全岩 $\varepsilon_{Nd}(t)$ 值应为 5.73～7.30,明显大于实际值,说明 Nd、Hf 同位素之间存在明显的解耦

现象.该现象在滇西马厂箐煌斑岩(贾丽琼等,2013)、鄂东南殷祖岩体(丁丽雪等,2017)、北山镁铁—超镁铁质岩(Su *et al*., 2015)及塔西南其木干玄武岩(李洪颜等,2013)中均有存在.

在 Rb-Sr、Sm-Nd 及 Lu-Hf 体系中,Rb、Sr 同属大离子亲石元素,Sm、Nd 同属稀土元素,Lu 属于稀土元素,而 Hf 属于高场强元素(吴福元等,2007).在洋壳俯冲过程中,稀土元素及大离子亲石元素在板片脱水流体中的活动性要明显大于高场强元素,流体携带 Nd 的能力要强于 Hf.因此,被这种流体交代过的地幔楔中会含有更多非放射成因的 Nd,而含有较少非放射成因的 Hf.使得流体交代地幔楔部分熔融形成的岩浆中 $\varepsilon_{Nd}(t)$ 值明显降低,而 $\varepsilon_{Hf}(t)$ 值变化不明显,从而导致 Nd-Hf 同位素解耦现象的出现(Pearce *et al*., 1999).如前文所述,玉海西闪长岩是由地幔楔部分熔融而形成的,俯冲板片脱水流体的交代可能是其 Nd-Hf 同位素解耦的原因.虽然玉海西辉长岩脉锆石 U-Pb 年龄及 Hf 同位素特征并未得到,其同样受到了板片脱水流体的交代,可能同样存在 $\varepsilon_{Nd}(t)$ 降低、单阶段 Nd 模式年龄增大和 Nd-Hf 同位素解耦的现象.Wang *et al*.(2018)指出,玉海矿区辉长岩脉与玉海西辉长岩脉有着相似的产状、矿物和地球化学成分,表明两者可能具有相似的源区和大地构造背景.然而,前者的 $\varepsilon_{Nd}(t)$ 和单阶段 Nd 模式年龄分别为 5.77～6.42 和 852～938 Ma;后者则显示较低的 $\varepsilon_{Nd}(t)$ 值(0.90～1.06)和较大的单阶段 Nd 模式年龄(1 305～1 342 Ma).这可能正是由板片脱水流体交代而引起的.玉海西片麻状花岗岩的 $\varepsilon_{Nd}(t)$ 值为 3.56～4.03,对应的模式年龄为 786～824 Ma,其锆石 $\varepsilon_{Hf}(t)$ 值为 10.8～14.2,对应的模式年龄为 458～667 Ma,Nd、Hf 同位素之间解耦现象不明显,这可能与片麻状花岗岩形成于新生下地壳,受板片脱水流体交代不明显相关.

5.4 构造环境

近些年来,前人在大南湖—头苏泉岛弧带及雅满苏—阿齐山带发现大量的泥盆纪到石炭纪岩浆岩,如大南湖二长花岗岩(383±9 Ma;宋彪等,2002)、咸水泉花岗闪长岩(369.5±5.6 Ma;唐俊华等,2007)、土屋—延东斜长花岗斑岩(339～332 Ma; Xiao *et al*., 2015; Shen *et al*., 2014a, 2014b)、三岔口东花岗质岩体(323～321 Ma;王超等,2015)、红云滩二长闪长岩(351.5±1.2 Ma;郑仁乔,2015)、西凤山钾长花岗岩(349.0±3.4 Ma;徐璐璐等,2014)、百灵山花岗质岩石(318～307 Ma; Zhang *et al*., 2016b)等.前人研究表明,这些岩体主要显示钙碱性、偏铝质特征,富集 LILEs 和 LILEs(如 Sr、Ba 等),亏损 HREEs 和 HFSEs(如 Nb、Ta 和 Ti 等),属于岛弧岩浆岩(Xiao *et al*., 2004; Wang *et al*., 2018),这些表明在泥盆纪—石炭纪时期,东天山古亚洲洋可能发生了双向俯冲,即:向北俯冲到大南湖—头苏泉岛弧带下,向南俯冲到阿齐山—雅满苏带下(Xiao *et al*., 2004; Wang *et al*., 2016a; Wang *et al*., 2018).期间,在大南湖—头苏泉岛弧带主要形成斑岩 Cu-Mo 矿,如土屋—延东(Xiao *et al*., 2015; Wang *et al*., 2018)、福兴(Wang *et al*., 2016c)及赤湖(Zhang *et al*., 2016a)等;在阿齐山—雅满苏带主要形成 Fe-Cu 矿,如百灵山(Zhang *et al*., 2016b)、黑尖山(Zhao *et al*., 2018)等.在约 364 Ma 时,古亚洲洋板片向大南湖—头苏泉岛弧带之下俯冲,导致大南湖岛弧带下新生下地壳部分熔融形成了玉海西花岗岩.

Zhang *et al*.(2002)在对康古尔—黄山韧性剪切带中康古尔造山型金矿的研究中指出,大南湖—头苏泉岛弧带与阿齐山—雅满苏带的碰撞发生在 300～290 Ma.近年来,人们在东天山地区及其周边发现了早二叠纪双峰式岩浆岩,如白杨沟岩体(296～293 Ma; Shu *et al*., 2010; Chen *et al*., 2011)、车轱辘泉岩体(295～294 Ma;陈希节和舒良树,2010; Yuan *et al*., 2010).这些岩体均形成于碰撞后伸展环境下,表明碰撞阶段发生在约 295 Ma 之前.

玉海西闪长岩具有较高的 Th/Yb 比值,相对较低的 Nb/Yb 比值,具有明显的俯冲带岛弧特征(图 10b,10c).在图 7a 中,玉海西闪长岩同样具有岛弧岩浆岩的同位素特征.这些特征表明,玉海西闪长岩形成于俯冲环境下.在阿齐山—雅满苏带上,Zhang *et al*.(2016b)得到百灵山花岗岩年龄约为 307 Ma,Zhao *et al*.(2018)得到赤龙峰花岗闪长岩年龄约为 306 Ma.这些岩体均形成于俯冲环境下,且与玉海西闪长岩几乎同时形成,也暗示了玉海西岩体具有相似的形成环境.

玉海西辉长岩脉具有明显幔源成因特征,且具有与岛弧岩浆相似的同位素及微量元素特征.然而,前人研究表明,碰撞后伸展环境下形成的岩浆岩同样会具有与岛弧岩浆相似的地球化学特征(Aldanmaz *et al*., 2000; Song and Li, 2009).如上所述,玉海西辉长岩脉侵入到玉海西闪长岩中,与玉海辉石闪长岩脉具有相似的分布特征、地球化学成分,因此可以肯定其形成于 306 Ma 以后,且可能与

玉海辉石闪长岩脉(291±3 Ma; Wang *et al*., 2018)一样,形成于碰撞后伸展的构造环境下.此外,大量 290～270 Ma 的岩浆 Cu-Ni 硫化物矿床形成于碰撞后伸展环境下(Han *et al*., 2010; Qin *et al*., 2011; Su *et al*., 2013),表明在～295 Ma 以后,东天山地区已进入碰撞后伸展阶段.由此,笔者推测,玉海西辉长岩脉可能形成于碰撞后伸展环境下.

6　结论

(1)锆石 LA-ICP-MS 定年结果表明,玉海西片麻状花岗岩年龄为 364.2±5.0 Ma;闪长岩年龄为 306.2±5.0 Ma.

(2)全岩地球化学特征、Sr-Nd-Hf 同位素特征表明:玉海西片麻状花岗岩形成于新生下地壳的部分熔融;闪长岩及辉长岩脉形成于亏损地幔的部分熔融,并混染有地壳物质.

(3)玉海西片麻状花岗岩及闪长岩均形成于岛弧环境,是古亚洲洋板片向北俯冲的结果;辉长岩脉形成于碰撞后伸展环境中.

致谢:本次研究得到了中科院广州地球化学研究所陈华勇研究员、中山大学海洋学院李登峰教授、中科院广州地球化学研究所张乐博士、中科院地球化学研究所沈能平副研究员的帮助;审稿专家给论文提出了许多宝贵的意见;在此一并表示衷心感谢!

References

Aldanmaz, E., Pearce, J.A., Thirlwall, M.F., et al., 2000. Petrogenetic Evolution of Late Cenozoic, Post-Collision Volcanism in Western Anatolia, Turkey. *Journal of Volcanology and Geothermal Research*, 102(1－2): 67－95. https://doi.org/10.1016/S0377-0273(00)00182-7

Allen, M.B., Windley, B.F., Zhang, C., 1993. Palaeozoic Collisional Tectonics and Magmatism of the Chinese Tien Shan, Central Asia. *Tectonophysics*, 220(1－4): 89－115. https://doi.org/10.1016/0040-1951(93)90225-9

Anderson, D.L., 1983. Chemical Composition of the Mantle. *Journal of Geophysical Research: Solid Earth*, 88(S1): 41－52. https://doi.org/10.1029/jb088is01p00b41

Arculus, R.J., Powell, R., 1986. Source Component Mixing in the Regions of Arc Magma Generation. *Journal of Geophysical Research*, 91(B6): 5913－5926. https://doi.org/10.1029/jb091ib06p05913

Barbarin, B., 1999. A Review of the Relationships between Granitoid Types, Their Origins and Their Geodynamic Environments. *Lithos*, 46(3): 605－626. https://doi.org/10.1016/s0024-4937(98)00085-1

Bouvier, A., Vervoort, J.D., Patchett, P.J., 2008. The Lu-Hf and Sm-Nd Isotopic Composition of CHUR: Constraints from Unequilibrated Chondrites and Implications for the Bulk Composition of Terrestrial Planets. *Earth and Planetary Science Letters*, 273(1－2): 48－57. https://doi.org/10.1016/j.epsl.2008.06.010

Cao, F.G., Tu, Q.J., Zhang, X.M., et al., 2006. Preliminary Determination of the Early Paleozoic Magmatic Arc in the Karlik Mountains, East Tianshan, Xinjiang, China—Evidence from Zircon SHRIMP U-Pb Dating of Granite Bodies in the Tashuihe Area. *Geological Bulletin of China*, 25(8): 923－927 (in Chinese with English abstract).

Chappell, B.W., White, A.J.R., Chappell, B., et al., 1974. Two Contrasting Granite Types. *Pacific Geology*, 8: 173－174.

Chen, X.J., Shu, L.S., Santosh, M., 2011. Late Paleozoic Post-Collisional Magmatism in the Eastern Tianshan Belt, Northwest China: New Insights from Geochemistry, Geochronology and Petrology of Bimodal Volcanic Rocks. *Lithos*, 127(3－4): 581－598. https://doi.org/10.1016/j.lithos.2011.06.008

Chen, X.J., Shu, L.S., 2010. Features of the Post-Collisional Tectono-Magmatism and Geochronological Evidence in the Harlik Mt., Xinjiang. *Acta Petrologica Sinica*, 26(10): 3057－3064 (in Chinese with English abstract).

Chen, Y.J., Chen, H.Y., Zaw, K., et al., 2007. Geodynamic Settings and Tectonic Model of Skarn Gold Deposits in China: An Overview. *Ore Geology Reviews*, 31(1－4): 139－169. https://doi.org/10.1016/j.oregeorev.2005.01.001

Chen, Y.J., Pirajno, F., Wu, G., et al., 2012. Epithermal Deposits in North Xinjiang, NW China. *International Journal of Earth Sciences*, 101(4): 889－917. https://doi.org/10.1007/s00531-011-0689-4

Collerson, K.D., Kamber, B.S., Schoenberg, R., 2002. Applications of Accurate, High-Precision Pb Isotope Ratio Measurement by Multi-Collector ICP-MS. *Chemical Geology*, 188(1－2): 65－83. https://doi.org/10.1016/s0009-2541(02)00059-1

Deng, X.H., Chen, Y.J., Santosh, M., et al., 2017. U-Pb Zircon, Re-Os Molybdenite Geochronology and Rb-Sr Geochemistry from the Xiaobaishitou W (-Mo) Deposit: Implications for Triassic Tectonic Setting in Eastern Tianshan, NW China. *Ore Geology Reviews*, 80: 332－351. https://doi.org/10.1016/j.oregeorev.2016.05.013

Ding, L.X., Huang, G.C., Xia, J.L., et al., 2017. Petrogenesis and Implications of the Yinzu Pluton in Southeast Hubei Province: Evidence from Geochronology, Geochem-

istry, and Sr-Nd-Hf Isotopes. *Acta Geologica Sinica*, 91(2): 362－383 (in Chinese with English abstract).

Gao, J. F., Zhou, M. F., Qi, L., et al., 2015. Chalcophile Elemental Compositions and Origin of the Tuwu Porphyry Cu Deposit, NW China. *Ore Geology Reviews*, 66: 403－421. https://doi.org/10.1016/j.oregeorev.2014.08.009

Green, T. H., 1995. Significance of Nb/Ta as an Indicator of Geochemical Processes in the Crust-Mantle System. *Chemical Geology*, 120(3－4): 347－359. https://doi.org/10.1016/0009-2541(94)00145-x

Griffin, W. L., Belousova, E. A., Shee, S. R., et al., 2004. Archean Crustal Evolution in the Northern Yilgarn Craton: U-Pb and Hf-Isotope Evidence from Detrital Zircons. *Precambrian Research*, 131(3－4): 231－282. https://doi.org/10.1016/j.precamres.2003.12.011

Griffin, W. L., Wang, X., Jackson, S. E., et al., 2002. Zircon Chemistry and Magma Mixing, SE China: In-Situ Analysis of Hf Isotopes, Tonglu and Pingtan Igneous Complexes. *Lithos*, 61(3－4): 237－269. https://doi.org/10.1016/s0024-4937(02)00082-8

Guo, H. C., Zhong, L., Li, L. Q., et al., 2006. Zircon SHRIMP U-Pb Dating of Quartz Diorite in the Koumenzi Area, Karlik Mountains, East Tianshan, Xinjiang, China, and Its Geological Significance. *Geological Bulletin of China*, 25(8): 928－931 (in Chinese with English abstract).

Guo, Q. Q., Pan, C. Z., Xiao, W. J., et al., 2010. Geological and Geochemical Characteristics of the Yandong Porphyry Copper Deposits in Hami, Xinjiang. *Xinjiang Geology*, 28(4): 419－426 (in Chinese with English abstract).

Han, C. M., Xiao, W. J., Zhao, G. C., et al., 2010. In-Situ U-Pb, Hf and Re-Os Isotopic Analyses of the Xiangshan Ni-Cu-Co Deposit in Eastern Tianshan (Xinjiang), Central Asia Orogenic Belt: Constraints on the Timing and Genesis of the Mineralization. *Lithos*, 120(3－4): 547－562. https://doi.org/10.1016/j.lithos.2010.09.019

Harris, N. B. W., Pearce, J. A., Tindle, A. G., 1986. Geochemical Characteristics of Collision-Zone Magmatism. *Geological Society, London, Special Publications*, 19(1): 67－81. https://doi.org/10.1144/gsl.sp.1986.019.01.04

Hofmann, A. W., 1997. Mantle Geochemistry: The Message from Oceanic Volcanism. *Nature*, 385(6613): 219－229. https://doi.org/10.1038/385219a0

Hou, T., Zhang, Z. C., Santosh, M., et al., 2014. Geochronology and Geochemistry of Submarine Volcanic Rocks in the Yamansu Iron Deposit, Eastern Tianshan Mountains, NW China: Constraints on the Metallogenesis. *Ore Geology Reviews*, 56: 487－502. https://doi.org/10.1016/j.oregeorev.2013.03.008

Hua, L. B., 2001. Element Geochemistry Subarea and Ore-Finding Direction of Metallogenic District, Yamansu-Shaquanzi, Eastern Tianshan, Xinjiang. *Journal of Guilin Institute of Technology*, 21(2): 99－103 (in Chinese with English abstract).

Jahn, B. M., Zhang, Z. Q., 1984. Archean Granulite Gneisses from Eastern Hebei Province, China: Rare Earth Geochemistry and Tectonic Implications. *Contributions to Mineralogy and Petrology*, 85(3): 224－243. https://doi.org/10.1007/bf00378102

Jia, L. Q., Mo, X. X., Dong, G. C., et al., 2013. Genesis of Lamprophyres from Machangqing, Western Yunnan: Constraints from Geochemistry, Geochronology and Sr-Nd-Pb-Hf Isotopes. *Acta Petrologica Sinica*, 29(4): 1247－1260 (in Chinese with English abstract).

Kepezhinskas, P., McDermott, F., Defant, M. J., et al., 1997. Trace Element and Sr-Nd-Pb Isotopic Constraints on a Three-Component Model of Kamchatka Arc Petrogenesis. *Geochimica et Cosmochimica Acta*, 61(3): 577－600. https://doi.org/10.1016/s0016-7037(96)00349-3

Li, B. P., Greig, A., Zhao, J. X., et al., 2005. ICP-MS Trace Element Analysis of Song Dynasty Porcelains from Ding, Jiexiu and Guantai Kilns, North China. *Journal of Archaeological Science*, 32(2): 251－259. https://doi.org/10.1016/j.jas.2004.09.004

Li, C., Qu, W. J., Du, A. D., et al., 2009. Decoupling of Re and Os and Migration Model of ^{187}Os in Coarse-Grained Molybdenite. *Mineral Deposits*, 28(5): 707－712 (in Chinese with English abstract).

Li, H. Q., 2004. Isotope Geochronology of Regional Mineralization in Xinjiang, NW China. Geological Publishing House, Beijing (in Chinese).

Li, H. Q., Chen, F. W., Li, J. Y., et al., 2006. Age of Mineralization and Host Rocks in the Baishan Rhenium-Molybdenum District, East Tianshan, Xinjiang, China: Revisited. *Geological Bulletin of China*, 25(8): 916－922 (in Chinese with English abstract).

Li, H. Q., Chen, F. W., Lu, Y. F., et al., 2004. Zircon SHRIMP U-Pb Age and Strontium Isotopes of Mineralized Granitoids in the Sanchakou Copper Polymetallic Depoist, East Tianshan Mountains. *Acta Geoscientica Sinica*, 25(2): 191－195 (in Chinese with English abstract).

Li, H. Y., Huang, X. L., Li, W. X., et al., 2013. Age and Geochemistry of the Early Permian Basalts from Qimugan in the Southwestern Tarim Basin. *Acta Petrologica Sinica*, 29(10): 3353－3368 (in Chinese with English abstract).

Li, W., Chen, J. L., Dong, Y. P., et al., 2016. Early Paleozoic Subduction of the Paleo-Asian Ocean: Zircon U-Pb Geo-

chronological and Geochemical Evidence from the Kalatag High-Mg Andesites, East Tianshan. *Acta Petrologica Sinica*, 32(2): 505 - 521 (in Chinese with English abstract).

Li, W.M., Ren, B.C., Yang, X.K., et al., 2002. The Intermediate-Acid Intrusive Magmatism and Its Geodynamic Significance in Eastern Tianshan Region. *Northwestern Geology*, 35(4): 41-64 (in Chinese with English abstract).

Liu, M., Wang, Z.L., Zhang, Z.H., et al., 2009. Fluid Inclusion Geochemistry of Tuwu Porphyry Copper Deposit, Eastern Tianshan in Xinjiang. *Acta Petrologica Sinica*, 25(6): 1446-1455 (in Chinese with English abstract).

Ma, X.H., Chen, B., Wang, C., et al., 2015. Early Paleozoic Subduction of the Paleo-Asian Ocean: Zircon U-Pb Geochronological, Geochemical and Sr-Nd Isotopic Evidence from the Harlik Pluton, Xinjiang. *Acta Petrologica Sinica*, 31(1): 89-104 (in Chinese with English abstract).

Maniar, P.D., Piccoli, P.M., 1989. Tectonic Discrimination of Granitoids. *Geological Society of America Bulletin*, 101(5): 635-643. https://doi.org/10.1130/0016-7606(1989)101<0635:tdog>2.3.co;2

Mao, J.W., Pirajno, F., Zhang, Z.H., et al., 2008. A Review of the Cu-Ni Sulphide Deposits in the Chinese Tianshan and Altay Orogens (Xinjiang Autonomous Region, NW China): Principal Characteristics and Ore-Forming Processes. *Journal of Asian Earth Sciences*, 32(2-4): 184-203. https://doi.org/10.1016/j.jseaes.2007.10.006

Mao, J.W., Goldfarb, R., Wang, Y.T., et al., 2005. Late Paleozoic Base and Precious Metal Deposits, East Tianshan, Xinjiang, China: Characteristics and Geodynamic Setting. *Episodes*, 28: 1-14.

McKenzie, D., 1989. Some Remarks on the Movement of Small Melt Fractions in the Mantle. *Earth and Planetary Science Letters*, 95(1-2): 53-72. https://doi.org/10.1016/0012-821x(89)90167-2

Meng, Q.R., 2003. What Drove Late Mesozoic Extension of the Northern China-Mongolia Tract? *Tectonophysics*, 369(3-4): 155-174. https://doi.org/10.1016/s0040-1951(03)00195-1

Mišković, A., Schaltegger, U., 2009. Crustal Growth along a Non-Collisional Cratonic Margin: A Lu-Hf Isotopic Survey of the Eastern Cordilleran Granitoids of Peru. *Earth and Planetary Science Letters*, 279(3-4): 303-315. https://doi.org/10.1016/j.epsl.2009.01.002

Morris, J.D., Hart, S.R., 1983. Isotopic and Incompatible Element Constraints on the Genesis of Island Arc Volcanics from Cold Bay and Amak Island, Aleutians, and Implications for Mantle Structure: Reply to a Critical Comment by M.R. Perfit and R.W. Kay. *Geochimica et Cosmochimica Acta*, 50(3): 483-487. https://doi.org/10.1016/0016-7037(86)90202-4

Pearce, J.A., Baker, P.E., Harvey, P.K., et al., 1995. Geochemical Evidence for Subduction Fluxes, Mantle Melting and Fractional Crystallization beneath the South Sandwich Island Arc. *Journal of Petrology*, 36(4): 1073-1109. https://doi.org/10.1093/petrology/36.4.1073

Pearce, J.A., Harris, N.B.W., Tindle, A.G., 1984. Trace Element Discrimination Diagrams for the Tectonic Interpretation of Granitic Rocks. *Journal of Petrology*, 25(4): 956-983. https://doi.org/10.1093/petrology/25.4.956

Pearce, J.A., Kempton, P.D., Nowell, G.M., et al., 1999. Hf-Nd Element and Isotope Perspective on the Nature and Provenance of Mantle and Subduction Components in Western Pacific Arc-Basin Systems. *Journal of Petrology*, 40(11): 1579-1611. https://doi.org/10.1093/petroj/40.11.1579

Peccerillo, A., Taylor, S.R., 1976. Geochemistry of Eocene Calc-Alkaline Volcanic Rocks from the Kastamonu Area, Northern Turkey. *Contributions to Mineralogy and Petrology*, 58(1): 63-81. https://doi.org/10.1007/bf00384745

Pirajno, F., 2009. Hydrothermal Processes and Mineral Systems. Springer, Berlin. https://doi.org/10.1007/978-1-4020-8613-7

Pirajno, F., 2013. The Geology and Tectonic Settings of China's Mineral Deposits. Springer, Berlin. https://doi.org/10.1007/978-94-007-4444-8_7

Plank, T., Langmuir, C.H., 1998. The Chemical Composition of Subducting Sediment and Its Consequences for the Crust and Mantle. *Chemical Geology*, 145(3/4): 325-394. https://doi.org/10.1016/s0009-2541(97)00150-2

Qin, K.Z., Fang, T.H., Wang, S.L., et al., 2002. Plate Tectonics Division, Evolution and Metallogenic Settings in Eastern Tianshan Mountains, NW-China. *Xinjiang Geology*, 20(4): 302-308 (in Chinese with English abstract).

Qin, K.Z., Su, B.X., Sakyi, P.A., et al., 2011. SIMS Zircon U-Pb Geochronology and Sr-Nd Isotopes of Ni-Cu-Bearing Mafic-Ultramafic Intrusions in Eastern Tianshan and Beishan in Correlation with Flood Basalts in Tarim Basin (NW China): Constraints on a ca. 280 Ma Mantle Plume. *American Journal of Science*, 311(3): 237-260. https://doi.org/10.2475/03.2011.03

Rapp, R.P., Watson, E.B., 1995. Dehydration Melting of Metabasalt at 8-32 kbar: Implications for Continental Growth and Crust-Mantle Recycling. *Journal of Petrology*, 36(4): 891-931. https://doi.org/10.1093/petrol-

ogy/36.4.891

Richards, J.P., Kerrich, R., 2007. Special Paper: Adakite-Like Rocks: Their Diverse Origins and Questionable Role in Metallogenesis. *Economic Geology*, 102(4): 537－576. https://doi.org/10.2113/gsecongeo.102.4.537

Rudnich, R.L., Gao, S., 2003. Composition of the Continental Crust. *Treatise on Geochemistry*, 3: 1－64. https://doi.org/ 10.1016/B0-08-043751-6/03016-4

Rui, Z.Y., Liu, Y.L., Wang, L.S., et al., 2002. The Eastern Tianshan Porphyry Copper Belt in Xinjiang and Its Tectonic Framework. *Acta Geologica Sinica*, 76(1): 83－94 (in Chinese with English abstract).

Shen, P., Pan, H.D., Cao, C., et al., 2017. The Formation of the Suyunhe Large Porphyry Mo Deposit in the West Junggar Terrain, NW China: Zircon U-Pb Age, Geochemistry and Sr-Nd-Hf Isotopic Results. *Ore Geology Reviews*, 81: 808－828. https://doi.org/10.1016/j.oregeorev.2016.02.015

Shen, P., Pan, H.D., Dong, L.H., 2014a. Yandong Porphyry Cu Deposit, Xinjiang, China—Geology, Geochemistry and SIMS U-Pb Zircon Geochronology of Host Porphyries and Associated Alteration and Mineralization. *Journal of Asian Earth Sciences*, 80: 197－217. https://doi.org/10.1016/j.jseaes.2013.11.006

Shen, P., Pan, H.D., Zhou, T.F., et al., 2014b. Petrography, Geochemistry and Geochronology of the Host Porphyries and Associated Alteration at the Tuwu Cu Deposit, NW China: A Case for Increased Depositional Efficiency by Reaction with Mafic Hostrock? *Mineralium Deposita*, 49(6): 709－731. https://doi.org/10.1007/s00126-014-0517-4

Shu, L.S., Wang, B., Zhu, W.B., et al., 2010. Timing of Initiation of Extension in the Tianshan, Based on Structural, Geochemical and Geochronological Analyses of Bimodal Volcanism and Olistostrome in the Bogda Shan (NW China). *International Journal of Earth Sciences*, 100(7): 1647－1663. https://doi.org/10.1007/s00531-010-0575-5

Smithies, R.H., Champion, D.C., 2000. The Archaean High-Mg Diorite Suite: Links to Tonalite-Trondhjemite-Granodiorite Magmatism and Implications for Early Archaean Crustal Growth. *Journal of Petrology*, 41(12): 1653－1671. https://doi.org/10.1093/petrology/41.12.1653

Söderlund, U., Patchett, P.J., Vervoort, J.D., et al., 2004. The ^{176}Lu Decay Constant Determined by Lu-Hf and U-Pb Isotope Systematics of Precambrian Mafic Intrusions. *Earth and Planetary Science Letters*, 219(3－4): 311－324. https://doi.org/10.1016/s0012-821x(04)00012-3

Song, B., Li, J.Z., Li, W.Q., et al., 2002. Shrimp Dating of Zircons from Dananhu and Kezirkalasayi Granitoid Batholith in Southern Margin of Tuha Basin and Their Geological Implication. *Xinjiang Geology*, 20 (4): 342－345 (in Chinese with English abstract).

Song, X.Y., Li, X.R., 2009. Geochemistry of the Kalatongke Ni-Cu-(PGE) Sulfide Deposit, NW China: Implications for the Formation of Magmatic Sulfide Mineralization in a Postcollisional Environment. *Mineralium Deposita*, 44(3): 303－327. https://doi.org/10.1007/s00126-008-0219-x

Su, B.X., Qin, K.Z., Lu, Y.H., et al., 2015. Decoupling of Whole-Rock Nd-Hf and Zircon Hf-O Isotopic Compositions of a 284 Ma Mafic-Ultramafic Intrusion in the Beishan Terrane, NW China. *International Journal of Earth Sciences*, 104(7): 1721－1737. https://doi.org/10.1007/s00531-015-1168-0

Su, B.X., Qin, K.Z., Tang, D.M., et al., 2013. Late Paleozoic Mafic-Ultramafic Intrusions in Southern Central Asian Orogenic Belt (NW China): Insight into Magmatic Ni-Cu Sulfide Mineralization in Orogenic Setting. *Ore Geology Reviews*, 51: 57－73. https://doi.org/10.1016/j.oregeorev.2012.11.007

Sun, S.S., McDonough, W.F., 1989. Chemical and Isotopic Systematics of Oceanic Basalts: Implications for Mantle Composition and Processes. *Geological Society, London, Special Publications*, 42(1): 313－345. https://doi.org/10.1144/gsl.sp.1989.042.01.19

Tang, J.H., Gu, L.X., Zhang, Z.Z., et al., 2007. Characteristics, Age and Origin of the Xianshuiquan Gneissose Granite in Eastern Tianshan. *Acta Petrologica Sinica*, 23(8): 1803－1820 (in Chinese with English abstract).

Vervoort, J.D., Blichert-Toft, J., 1999. Evolution of the Depleted Mantle: Hf Isotope Evidence from Juvenile Rocks through Time. *Geochimica et Cosmochimica Acta*, 63(3－4): 533－556. https://doi.org/10.1016/s0016-7037(98)00274-9

Wang, C., Chen, B., Ma, X.H., et al., 2015. Petrogenesis of Early and Late Paleozoic Plutons in Sanchakou Area of East Tianshan and Their Implications for Evolution of Kangur Suture Zone. *Journal of Earth Sciences and Environment*, 37(5): 52－70 (in Chinese with English abstract).

Wang, J.B., Wang, Y.W., He, Z.J., et al., 2006. Ore Deposits as a Guide to the Tectonic Evolution in the East Tianshan Mountains, NW China. *Geology in China*, 33(3): 461－469 (in Chinese with English abstract).

Wang, J.B., Xu, X., 2006. Post-Collisional Tectonic Evolution and Metallogenesis in Northern Xinjiang, China. *Acta Geologica Sinica*, 80(1): 23－31 (in Chinese with English abstract).

Wang, Y.F., Chen, H.Y., Han, J.S., et al., 2018. Paleozoic Tectonic Evolution of the Dananhu-Tousuquan Island Arc Belt, Eastern Tianshan: Constraints from the Magmatism of the

Yuhai Porphyry Cu Deposit, Xinjiang, NW China. *Journal of Asian Earth Sciences*, 153: 282－306. https://doi.org/10.1016/j.jseaes.2017.05.022

Wang, Y. F., Chen, H. Y., Xiao, B., et al., 2016. Porphyritic-Overlapped Mineralization of Tuwu and Yandong Copper Deposits in Eastern Tianshan Mountains, Xinjiang. *Mineral Deposits*, 35(1): 51－68 (in Chinese with English abstract).

Wang, Y.F., Chen, H. Y., Xiao, B., et al., 2017. Overprinting Mineralization in the Paleozoic Yandong Porphyry Copper Deposit, Eastern Tianshan, NW China—Evidence from Geology, Fluid Inclusions and Geochronology. *Ore Geology Reviews*, Online. https:// doi. org/10. 1016/j. oregeorev.2017.04.013

Wang, Y.H., Zhang, F.F., 2016a. Petrogenesis of Early Silurian Intrusions in the Sanchakou Area of Eastern Tianshan, Northwest China, and Tectonic Implications: Geochronological, Geochemical, and Hf Isotopic Evidence. *International Geology Review*, 58(10): 1294－1310. https://doi.org/10.1080/00206814.2016.1152516

Wang, Y.H., Zhang, F.F., Liu, J.J., 2016b. The Genesis of the Ores and Intrusions at the Yuhai Cu-Mo Deposit in Eastern Tianshan, NW China: Constraints from Geology, Geochronology, Geochemistry, and Hf Isotope Systematics. *Ore Geology Reviews*, 77: 312－331. https://doi.org/10.1016/j.oregeorev.2016.03.003

Wang, Y. H., Zhang, F. F., Liu, J. J., et al., 2016c. Genesis of the Fuxing Porphyry Cu Deposit in Eastern Tianshan, China: Evidence from Fluid Inclusions and C-H-O-S-Pb Isotope Systematics. *Ore Geology Reviews*, 79: 46－61. https://doi.org/10.1016/j.oregeorev.2016.04.022

Wang, Y. H., Xue, C. J., Liu, J. J., et al., 2014. Geochemistry, Geochronology, Hf Isotope, and Geological Significance of the Tuwu Porphyry Copper Deposit in Tianshan, Xinjiang. *Acta Petrologica Sinica*, 30(11): 3383－3399 (in Chinese with English abstract).

Wedepohl, K. H., 1995. The Composition of the Continental Crust. *Geochimica et Cosmochimica Acta*, 59: 1217－1232. https://doi.org/10.1016/0016-7037(95)00038-2

Whalen, J. B., Currie, K. L., Chappell, B. W., 1987. A-Type Granites: Geochemical Characteristics, Discrimination and Petrogenesis. *Contributions to Mineralogy and Petrology*, 95(4): 407－419. https:// doi. org/10. 1007/bf00402202

Wu, F.Y., Li, X.H., Zheng, Y.F., et al., 2007. Lu-Hf Isotopic Systematics and Their Applications in Petrology. *Acta Petrologica Sinica*, 23(2): 185－220 (in Chinese with English abstract).

Wu, F.Y., Sun, D.Y., Ge, W.C., et al., 2011. Geochronology of the Phanerozoic Granitoids in Northeastern China. *Journal of Asian Earth Sciences*, 41(1): 1－30. https://doi.org/10.1016/j.jseaes.2010.11.014

Wu, F.Y., Sun, D.Y., Li, H.M., et al., 2002. A-Type Granites in Northeastern China: Age and Geochemical Constraints on Their Petrogenesis. *Chemical Geology*, 187(1－2): 143－173. https://doi.org/10.1016/s0009-2541(02)00018-9

Wu, Y. S., Xiang, N., Tang, S. H., et al., 2013. Molybdenite Re-Os Isotope Age of the Donggebi Mo Deposit and the Indosinian Metallogenic Event in Eastern Tianshan. *Acta Petrologica Sinica*, 29(1): 121－130 (in Chinese with English abstract).

Xiao, B., Chen, H. Y., Hollings, P., et al., 2015. Magmatic Evolution of the Tuwu-Yandong Porphyry Cu Belt, NW China: Constraints from Geochronology, Geochemistry and Sr-Nd-Hf Isotopes. *Gondwana Research*, 43: 74－91. https://doi.org/10.1016/j.gr.2015.09.003

Xiao, B., Chen, H. Y., Wang, Y. F., et al., 2015. Discovery of the Late Silurian Granodiorite and Its Tectonic Significance in the Tuwu-Yandong Porphyry Copper Deposits, Dananhu-Tousuquan Island Arc, Eastern Tianshan. *Earth Science Frontiers*, 22(6): 251－266 (in Chinese with English abstract).

Xiao, B., Chen, H. Y., Wang, Y. F., et al., 2017. Zircon U-Pb and Molybdenite Re-Os Dating of the Tuwu-Yandong Cu Deposit Belt of the Eastern Tianshan Mountains and Its Geological Significance. *Geotectonica et Metallogenia*, 41(1): 145－156 (in Chinese with English abstract).

Xiao, W.J., Windley, B.F., Allen, M.B., et al., 2013. Paleozoic Multiple Accretionary and Collisional Tectonics of the Chinese Tianshan Orogenic Collage. *Gondwana Research*, 23(4): 1316－1341. https://doi.org/10.1016/j.gr.2012.01.012

Xiao, W. J., Windley, B. F., Hao, J., et al., 2003. Accretion Leading to Collision and the Permian Solonker Suture, Inner Mongolia, China: Termination of the Central Asian Orogenic Belt. *Tectonics*, 22(6): 1069－1088. https://doi.org/10.1029/2002tc001484

Xiao, W.J., Zhang, L.C., Qin, K.Z., et al., 2004. Paleozoic Accretionary and Collisional Tectonics of the Eastern Tianshan (China): Implications for the Continental Growth of Central Asia. *American Journal of Science*, 304(4): 370－395. https://doi.org/10.2475/ajs.304.4.370

Xu, B., Charvet, J., Chen, Y., et al., 2013. Middle Paleozoic Convergent Orogenic Belts in Western Inner Mongolia (China): Framework, Kinematics, Geochronology and Implications for Tectonic Evolution of the Central Asian Orogenic Belt. *Gondwana Research*, 23(4): 1342－1364.

https://doi.org/10.1016/j.gr.2012.05.015

Xu, L. L., Chai, F. M., Li, Q., et al., 2014. Geochemistry and Zircon U-Pb Age of Volcanic Rocks from the Shaquanzi Fe-Cu Deposit in East Tianshan Mountains and Their Geological Significance. *Geology in China*, 41(6): 1771－1790 (in Chinese with English abstract).

Yuan, C., Sun, M., Wilde, S., et al., 2010. Post-Collisional Plutons in the Balikun Area, East Chinese Tianshan: Evolving Magmatism in Response to Extension and Slab Break-Off. *Lithos*, 119(3/4): 269－288. https://doi.org/10.1016/j.lithos.2010.07.004

Zhai, Y.S., Yao, S.Z., Cai, K.Q., 2011. Mineral Deposits (3rd Edition). Geological Publishing House, Beijing (in Chinese).

Zhang, D.Y., Zhou, T.F., Yuan, F., et al., 2010. Geochemical Characters, Metallogenic Chronology and Geological Significance of the Yanxi Copper Deposit in Eastern Tianshan, Xinjiang. *Acta Petrologica Sinica*, 26(11): 3327－3338 (in Chinese with English abstract).

Zhang, F.F., Wang, Y.H., Liu, J.J., et al., 2015. Zircon U-Pb and Molybdenite Re-Os Geochronology, Hf Isotope Analyses, and Whole-Rock Geochemistry of the Donggebi Mo Deposit, Eastern Tianshan, Northwest China, and Their Geological Significance. *International Geology Review*, 57(4): 446－462. https://doi.org/10.1080/00206814.2015.1013067

Zhang, F.F., Wang, Y.H., Liu, J.J., 2016a. Petrogenesis of Late Carboniferous Granitoids in the Chihu Area of Eastern Tianshan, Northwest China, and Tectonic Implications: Geochronological, Geochemical, and Zircon Hf-O Isotopic Constraints. *International Geology Review*, 58(8): 949－966. https://doi.org/10.1080/00206814.2015.1136800

Zhang, L.C., Liu, T.B., Shen, Y.C., et al., 2002. Isotopic Geochronology of the Late Paleozoic Kanggur Gold Deposit of East Tianshan Mountains, Xinjiang, NW China. *Resource Geology*, 52(3): 249－261. https://doi.org/10.1111/j.1751-3928.2002.tb00135.x

Zhang, L.C., Qin, K.Z., Xiao, W.J., 2008. Multiple Mineralization Events in the Eastern Tianshan District, NW China: Isotopic Geochronology and Geological Significance. *Journal of Asian Earth Sciences*, 32(2－4): 236－246. https://doi.org/10.1016/j.jseaes.2007.10.011

Zhang, L.C., Shen, Y.C., Ji, J.S., 2003. Characteristics and Genesis of Kanggur Gold Deposit in the Eastern Tianshan Mountains, NW China: Evidence from Geology, Isotope Distribution and Chronology. *Ore Geology Reviews*, 23(1－2): 71－90. https://doi.org/10.1016/s0169-1368(03)00016-7

Zhang, L.C., Xiao, W.J., Qin, K.Z., et al., 2004. Types, Geological Features and Geodynamic Significances of Gold-Copper Deposits in the Kanggurtag Metallogenic Belt, Eastern Tianshan, NW China. *International Journal of Earth Sciences*, 93(2): 224－240. https://doi.org/10.1007/s00531-004-0383-x

Zhang, L.C., Xiao, W.J., Qin, K.Z., et al., 2006. The Adakite Connection of the Tuwu-Yandong Copper Porphyry Belt, Eastern Tianshan, NW China: Trace Element and Sr-Nd-Pb Isotope Geochemistry. *Mineralium Deposita*, 41(2): 188－200. https://doi.org/10.1007/s00126-006-0058-6

Zhang, W.F., Chen, H.Y., Han, J.S., et al., 2016b. Geochronology and Geochemistry of Igneous Rocks in the Bailingshan Area: Implications for the Tectonic Setting of Late Paleozoic Magmatism and Iron Skarn Mineralization in the Eastern Tianshan, NW China. *Gondwana Research*, 38: 40－59. https://doi.org/10.1016/j.gr.2015.10.011

Zhang, Z.W., Zang, Y.S., Wang, Y.L., et al., 2016. Zircon SHRIMP U-Pb Age of the Yuhai Porphyry Copper Deposit in Eastern Tianshan Mountains of Xinjiang and Its Tectonic Implications. *Acta Geoscientica Sinica*, 37(1): 59－68 (in Chinese with English abstract).

Zhao, L.D., Chen, H.Y., Zhang, L., et al., 2018. The Late Paleozoic Magmatic Evolution of the Aqishan-Yamansu Belt, Eastern Tianshan: Constraints from Geochronology, Geochemistry and Sr-Nd-Pb-Hf Isotopes of Igneous Rocks. *Journal of Asian Earth Sciences*, 153: 170－192. https://doi.org/10.1016/j.jseaes.2017.07.038

Zheng, R.Q., 2015. Geological Characteristics and Genesis of Hongyuntan Iron Deposits in the Estern Tianshan, Xinjiang (Dissertation). China University of Geosciences, Beijing (in Chinese with English abstract).

Zhou, L.G., Xia, Q.X., Zheng, Y.F., et al., 2014. Polyphase Growth of Garnet in Eclogite from the Hong'an Orogen: Constraints from Garnet Zoning and Phase Equilibrium. *Lithos*, 206－207: 79－99. https://doi.org/10.1016/j.lithos.2014.06.020

Zhou, T.F., Yuan, F., Zhang, D.Y., et al., 2010. Geochronology, Tectonic Setting and Mineralization of Granitoids in Jueluotage Area, Eastern Tianshan, Xinjiang. *Acta Petrologica Sinica*, 26(2): 478－502 (in Chinese with English abstract).

Zhu, Y.F., An, F., Feng, W.Y., et al., 2016. Geological Evolution and Huge Ore-Forming Belts in the Core Part of the Central Asian Metallogenic Region. *Journal of Earth Science*, 27(3): 491－506. https://doi.org/10.1007/s12583-016-0673-7

附中文参考文献

曹福根,涂其军,张晓梅,任燕,等,2006.哈尔里克山早古生代岩浆弧的初步确定——来自塔水河一带花岗质岩体锆石 SHRIMP U-Pb 测年的证据.岩石学报,25(8):923－927.

陈希节,舒良树,2010.新疆哈尔里克山后碰撞期构造岩浆活动特征及年代学证据.岩石学报,26(10):3057－3064.

丁丽雪,黄圭成,夏金龙,等,2017.鄂东南地区殷祖岩体的成因及其地质意义:年代学、地球化学和 Sr-Nd-Hf 同位素证据.地质学报,91(2):362－383.

郭华春,钟莉,李丽群,等,2006.哈尔里克山口门子地区石英闪长岩锆石 SHRIMP U-Pb 测年及其地质意义.地质通报,25(8):928－931.

郭谦谦,潘成泽,肖文交,等,2010.哈密延东铜矿床地质和地球化学.新疆地质,28(4):419－426.

花林宝,2001.新疆东天山雅满苏－沙泉子成矿区元素地球化学分区及找矿方向.桂林工学院学报,21(2):99－103.

贾丽琼,莫宣学,董国臣,等,2013.滇西马厂箐煌斑岩成因:地球化学、年代学及 Sr-Nd-Pb-Hf 同位素约束.岩石学报,29(4):1247－1260.

李超,屈文俊,杜安道,等,2009.大颗粒辉钼矿 Re-Os 同位素使耦现象及 ^{187}Os 迁移模式研究.矿床地质,28(5):707－712.

李洪颜,黄小龙,李武显,等,2013.塔西南其木干早二叠世玄武岩的喷发时代及地球化学特征.岩石学报,29(10):3353－3368.

李华芹,2004.中国新疆区域成矿作用年代学.北京:地质出版社.

李华芹,陈富文,李锦轶,等,2006.再论东天山白山铼钼矿区成岩成矿时代.地质通报,25(8):916－922.

李华芹,陈富文,路远发,等,2004.东天山三岔口铜矿区矿化岩体 SHRIMP U-Pb 年代学及锶同位素地球化学特征研究.地球学报,25(2):191－195.

李玮,陈隽璐,董云鹏,等,2016.早古生代古亚洲洋俯冲记录:来自东天山卡拉塔格高镁安山岩的年代学、地球化学证据.岩石学报,32(2):505－521.

李文明,任秉琛,杨兴科,等,2002.东天山中酸性侵入岩浆作用及其地球动力学意义.西北地质,35(4):41－64.

刘敏,王志良,张作衡,等,2009.新疆东天山土屋斑岩铜矿流体包裹体地球化学特征.岩石学报,25(6):1446－1455.

马星华,陈斌,王超,等,2015.早古生代古亚洲洋俯冲作用:来自新疆哈尔里克侵入岩的锆石 U-Pb 年代学、岩石地球化学和 Sr-Nd 同位素证据.岩石学报,31(1):89－104.

秦克章,方同辉,王书来,等,2002.东天山板块构造分区、演化与成矿地质背景研究.新疆地质,20(4):302－308.

芮宗瑶,刘玉琳,王龙生,等,2002.新疆东天山斑岩型铜矿带及其大地构造格局.地质学报,76(1):83－94.

宋彪,李锦轶,李文铅,等,2002.吐哈盆地南缘克孜尔卡拉萨依和大南湖花岗质岩基锆石 SHRIMP 定年及其地质意义.新疆地质,20(4):342－345.

唐俊华,顾连兴,张遵忠,等,2007.东天山咸水泉片麻状花岗岩特征、年龄及成因.岩石学报,23(8):1803－1820.

王超,陈斌,马星华,等,2015.东天山三岔口地区早、晚古生代岩体成因及其对康古尔缝合带演化的意义.地球科学与环境学报,37(5):52－70.

王京彬,王玉往,何志军,等,2006.东天山大地构造演化的成矿示踪.中国地质,33(3):461－469.

王京彬,徐新,2006.新疆北部后碰撞构造演化与成矿.地质学报,80(1):23－31.

王银宏,薛春纪,刘家军,等,2014.新疆东天山土屋斑岩铜矿矿床地球、化学年代学、Lu-Hf 同位素及其地质意义.岩石学报,30(11):3383－3399.

王云峰,陈华勇,肖兵,等,2016.新疆东天山地区土屋和延东铜矿床斑岩－叠加改造成矿作用.矿床地质,35(1):51－68.

吴福元,李献华,郑永飞,等,2007.Lu-Hf 同位素体系及其岩石学应用.岩石学报,23(2):185－220.

吴艳爽,项楠,汤书好,等,2013.东天山东戈壁钼矿床辉钼矿 Re-Os 年龄及印支期成矿事件.岩石学报,29(1):121－130.

肖兵,陈华勇,王云峰,等,2015.东天山土屋－延东铜矿矿区晚志留世岩体的发现及构造意义.地学前缘,22(6):251－266.

肖兵,陈华勇,王云峰,等,2017.东天山土屋－延东铜矿带石英钠长斑岩与辉钼矿形成年龄及其重要意义.大地构造与成矿学,41(1):145－156.

徐璐璐,柴凤梅,李强,等,2014.东天山沙泉子铁铜矿区火山岩地球化学特征,锆石 U-Pb 年龄及地质意义.中国地质,41(6):1771－1790.

翟裕生,姚书振,蔡克勤,2011.矿床学(第三版).北京:地质出版社.

张达玉,周涛发,袁峰,等,2010.新疆东天山地区延西铜矿床的地球化学、成矿年代及其地质意义.岩石学报,26(11):3327－3338.

张照伟,臧遇时,王亚磊,等,2016.新疆东天山玉海斑岩铜矿锆石 SHRIMP U-Pb 年龄及构造意义.地球学报,37(1):59－68.

郑仁乔,2015.新疆东天山红云滩铁矿床地质特征与矿床成因研究(硕士学位论文).北京:中国地质大学.

周涛发,袁峰,张达玉,等,2010.新疆东天山觉罗塔格地区花岗岩类年代学、构造背景及其成矿作用研究.岩石学报,26(2):478－502.